Membrane Interactions of *Streptococcus agalactiae's* CAMP factor

By

David Donkor

A thesis

presented to the University of Waterloo

in fulfillment of the

thesis requirement for the degree of

Master of Science

in

Chemistry

Waterloo, Ontario, Canada, 2007

I hereby declare that I am the sole author of this thesis. This is a true copy of the thesis, including any required final revisions, as accepted by my examiners.

David Donkor

I understand that my thesis may be made electronically available to the public.

David Donkor

Abstract

CAMP factor is an extracellular pore-forming toxin secreted by the group B streptococci *Streptococcus agalactiae.* In conjunction with the action of sphingomyelinase secreted by *Staphylococcus aureus,* which converts membrane sphingomyline to ceramide, CAMP factor kills susceptible cells by creating holes in them.

Since the monomeric or oligomeric structure of CAMP factor is not yet known, no studies on the membrane-penetrating domain of this toxin have been done. In the present study, the interaction of a putative hydrophobic domain between residues T90 and V115 with the target membrane was examined by cysteine-scanning mutagenesis and site-selective fluorescent labeling.

The combination of steady state and lifetime fluorescence measurements and collisional quenching experiments with nitroxide labeled fatty acids indicate that residues from T90 to V115 contact the membrane upon binding and oligomerization of CAMP factor on cell membranes. More importantly, all these individual assays indicate that the residues from N104 to F109 insert superficially into the membrane with a β-sheet conformation.

Acknowledgements

I would like to express my appreciation to my supervisor, Dr. Micheal Palmer, for the opportunity he granted me to learn more about myself as a researcher, and to build myself as a scientist. I would also like to express my gratitude for his support, patience, and his many constructive criticisms.

I would also like to thank my committee members, Dr. John Honek and Dr. Guy Guillemette for their time spent in both my talks and their many questions regarding my work.

Last but not least, my appreciation goes to all my lab members, and all the friends I made in the Biochemistry department.

Table of Contents

List of Figures

List of Tables

List of Equations

Abbreviations

ADP: adenosine diphosphate

α-HL: Alpha hemolysin

BSA: bovine serum albumin

C: catalytic domain

CD: Circular dichroism

CBT: cholesterol binding toxin

DMF: dimethylformamide

DMSO: dimethyl sulphoxide

DSA: doxyl stearic acid

DNA: deoxyribonucleic acid

DTT: dithiothreitol

DT: diphtheria toxin

d NTP: deoxynucleoside triphosphate

EDTA: ethylene diaminotetraacetic acid

GBS: Group B Streptococcus

GST: glutathione-S-transferase

IPTG: isopropyl-β-D-thiogalactopyranoside

IAEDANDS: N-iodoacetyl-N-(5-sulfo-1-naphthyl)ethylenediamine

IANBD: N, N'-dimethyl-N- (iodoacetyl)-N'-(7-nitrobenz-2-oxa-1,3-diazol-4-yl)ethylenediamine

kDa: Kilo-Dalton

Leu: Leucine

LukF: Leukocidin F

LukS: Leukocidin S

Lys: Lysine

MW: molecular weight

OD: optical density

PA: anthrax toxin protective antigen

PCR: polymerase chain reaction

PEG: Polyethylene Glycol

PFT: Pore Forming Toxin

PFO: perfringolysin O

pI: Isoelectric Point

R: receptor binding domain

SDS-PAGE: sodium dodecyl sulfate polyacrylamide gel electrophoresis

SLO: Streptolysin O

T: transmembrane domain

1.0 INTRODUCTION

CAMP factor is an extra-cellular protein secreted by group B streptococci (GBS) or *Streptococcus agalactiae,* with a pI of 8.6 and a molecular mass of 25kDa. *Streptococcus agalactiae* is a major cause of mastitis in dairy cattle and a source of economic loss for the industry (*1*). *S. agalactiae* also causes neonatal septicemia in humans. Human infection is generally acquired from other human sources, although there may be some risk associated with direct exposure to infected animals or their products. Overall, there is considerable homology between strains isolated from septicemic infants and mastitic cows (*1*). *Streptococcus agalactiae* is now recognized to be part of the normal bacterial flora in the human throat, genitourinary tract, and rectum (*1*).

When grown on sheep blood agar plates next to a colony of *Staphylococcus aureus*, *Streptococcus agalactiae* induces a hemolytic phenomenon. This phenomenon was first described in 1944 by Christie, Atkins and Munch-Petersen, and thus named the CAMP reaction (*2*).

The CAMP reaction is widely used for the presumptive identification of *Streptococcus agalactiae* in clinical isolates. Typically, a nutrient sheep blood agar plate is used in this procedure (*1*). A strain of *Staphylococcus aureus* that produces sphingomyelinase (also known as β-hemolysin), and the putative isolates of *S. agalactiae* are streaked across a plate at right angles, close to but not touching each other. If CAMP factor is present, a distinct zone of hemolysis develops in the adjoining area of the two streaks where the red cells are exposed to both sphingomyelinase and CAMP factor (figure 1.1).

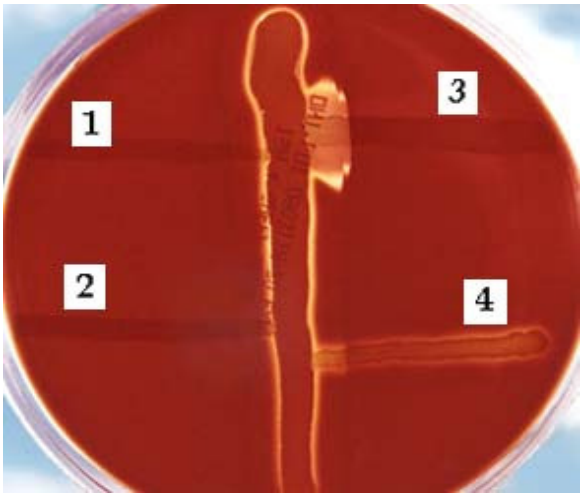

Figure 1.1: CAMP reaction. A blood agar plate is shown after 24 hours of incubation at 37°C. The vertical streak is a β-hemolysin-producing strain of *Staphylococcus aureus*, and at right angles to it are streaks of (1) *Enterococcus faecalis*, (2) *Streptococcus salivarius*, (3) *Streptococcus agalactiae*, and (4) *Enterococcus durans*. Note the large area of complete hemolysis where the extracellular compound of *S. agalactiae* encounters the β-hemolysin of *S. aureus* (*3*).

Bernheimer *et al*. were the first to intensively explore the nature and mechanism of the CAMP reaction. They purified CAMP factor from bacterial culture supernatants and determined the pI and molecular weight (*4*). They also pointed out the role of sphingomyelinase in the CAMP reaction, and the sequential nature of the latter (*4*). In the first step, sphingomyelin in the sheep red blood cell membranes is converted to ceramide (figure 1.2) by sphingomyelinase from *Staphylococcus aureus*. CAMP factor then binds to the pretreated cell membranes, leading to hemolysis of the cell.

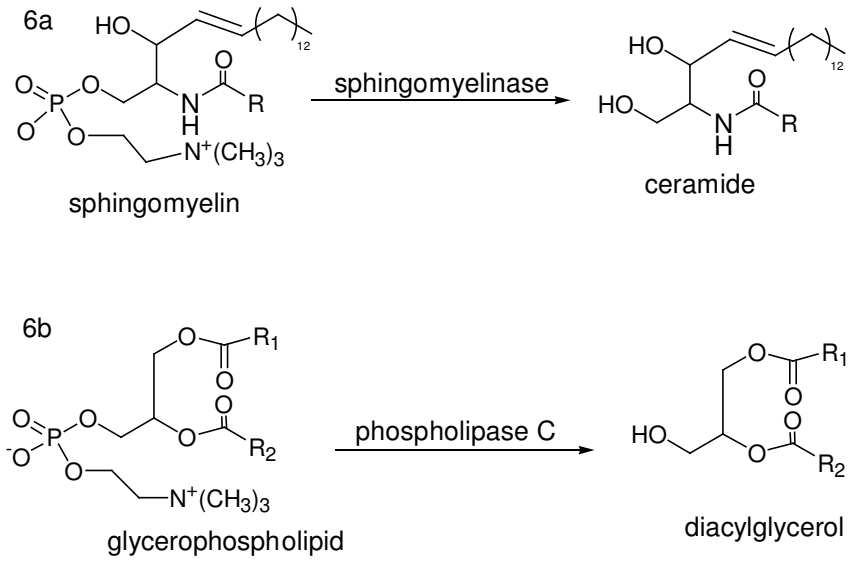

Figure 1.2: The reactions catalyzed by sphingomyelinase and phospholipase C.

Christie, Fehrenbach and co-workers reported that CAMP factor may cause lysis of red blood cells that contain at least 45 mol% of sphingomyelin in the cell membrane (*5*), (*6*). They demonstrated that sphingomyelinase-treated sheep and bovine erythrocytes, which contain 50 and 45 mol% of sphingomyelin respectively, are susceptible to CAMP factor; in contrast, human, horse, or rabbit erythrocytes, which contain less than 25 mol% sphingomyelin, are not susceptible (*7*). However, when human and rabbit erythrocytes were treated with phospholipase C, which will convert the glycerophospholipids to diacylglycerol (figure 1.2), the CAMP reaction could be observed (*8*). These results demonstrated that ceramide was not specifically required for the CAMP reaction. By using artificial membranes (liposomes), Fehrenbach and co-workers also showed that the cholesterol content in the target membrane was critical to CAMP factor activity (*6*), (*8*).

CAMP factor is a cysteine-free protein with two methionine residues. For the purpose of this study, the two methionine residues were substituted with leucine, forming

the double mutant CAMP^{M21L,M107L}, which was expressed as a 52 kDa glutathione-S-transferase fusion protein in *E. coli.* The fusion protein was purified to homogeneity using affinity chromatography and cleaved by thrombin to yield the recombinant 25 kDa CAMP factor protein. The resulting recombinant protein was shown to possess similar hemolytic activity to the native protein.

1.1 CAMP Factor is a Pore-Forming Toxin

The CAMP reaction shown above establishes that CAMP factor causes lysis of sphingomyelinase-treated sheep red blood cells. However, what is its mode of action? Electron microscopy and osmotic protection experiments using polyethylene glycol (PEG) by S. Lang and M. Palmer showed that CAMP factor forms pores of heterogeneous size on red blood cells (*9*). These pores are tiny holes admitting passage of liquids or ions, and while most of the pores created by CAMP factor are very small and sometimes hard to distinguish from the background, some pores are larger than 12 nm and with regular round shapes (figure 1.3 D) and irregular shapes (figures 1.3 B, and C).

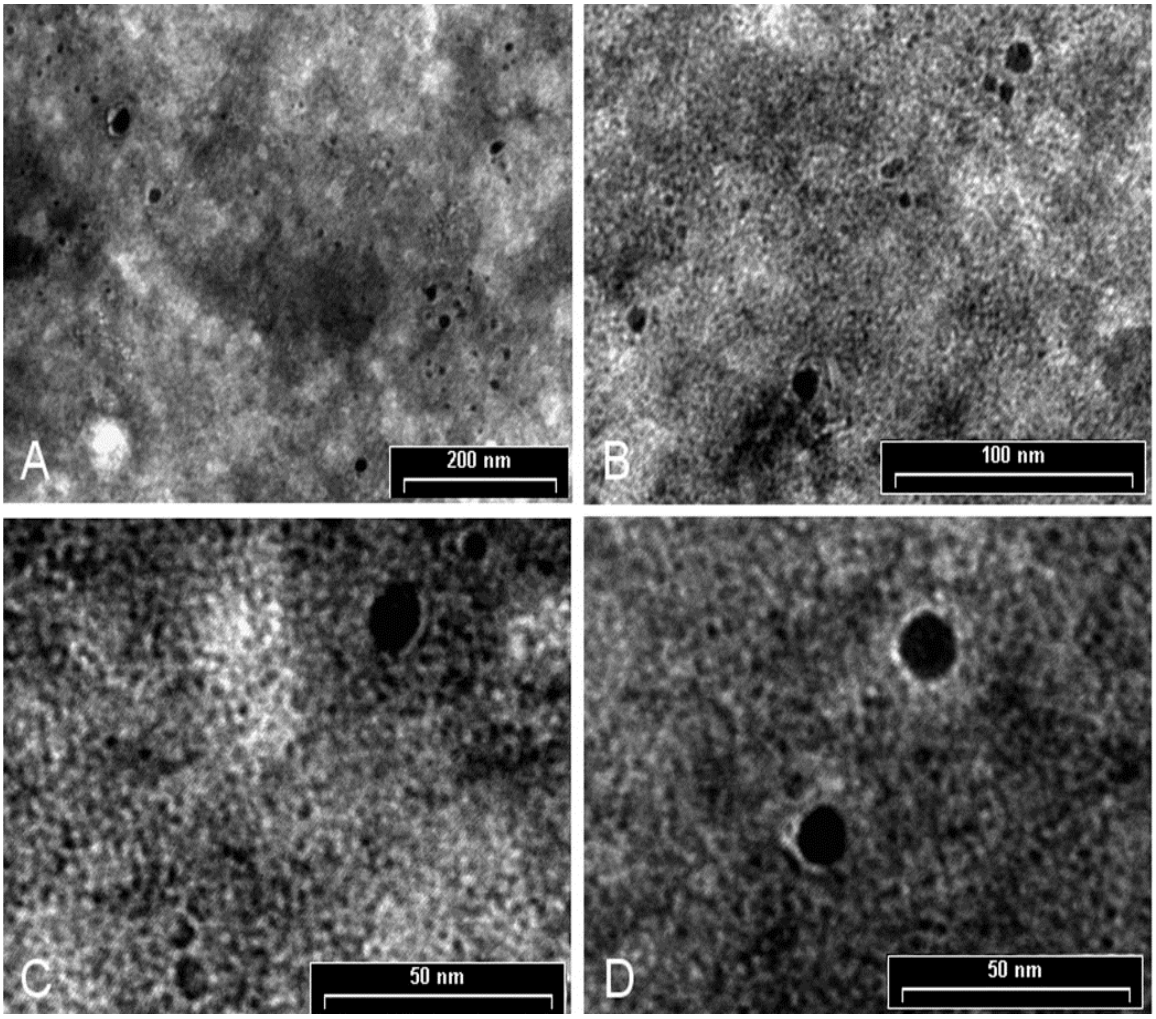

Figure 1.3: An electron micrograph of the pores on red blood cells. The pores range in sizes depending on the toxin concentration (*9*). Magnification varies among panels A-D by the *scale bars.*

In the osmotic protection experiments, there was a considerable delay of hemolysis in the presence of PEG 6000 and PEG 8000. Hemolysis was even much slower with PEG 10000. In contrast, PEG 1000 and PEG 4000 had no protective effect on CAMP factor-mediated hemolysis. When cells were incubated with CAMP factor in the presence of PEG 10000, washed twice in the same buffer to remove unbound protein, and re-suspended in buffer without PEG, hemolysis occurred immediately. This

confirmed that pore-formation had indeed proceeded in the presence of PEG, indicating that PEG had effected osmotic protection, but had not directly inhibited the binding or hemolytic action of CAMP factor. These data indicate that CAMP factor forms pores with a defined diameter on susceptible membranes (*9*).

1.2 Pore-Forming Toxins (PFTs)

The above experiments confirm the pore-forming characteristics of CAMP factor. Proteins and peptides with pore-forming activities are found in a variety of organisms such as bacteria, plants, fungi, primitive metazoans, insects and humans (*10*). Not all pore-forming proteins produced by these organisms are toxins however, and for the purpose of this study, only the toxins will be considered. Pore-forming toxins are mostly produced as water-soluble molecules destined to form pores in the lipid membranes of the host organism. They interact with cell or artificial lipid membranes, change conformation and oligomerize in the plane of the membrane to build water-filled pores that are permeable to solutes (*11*), figure 1.4.

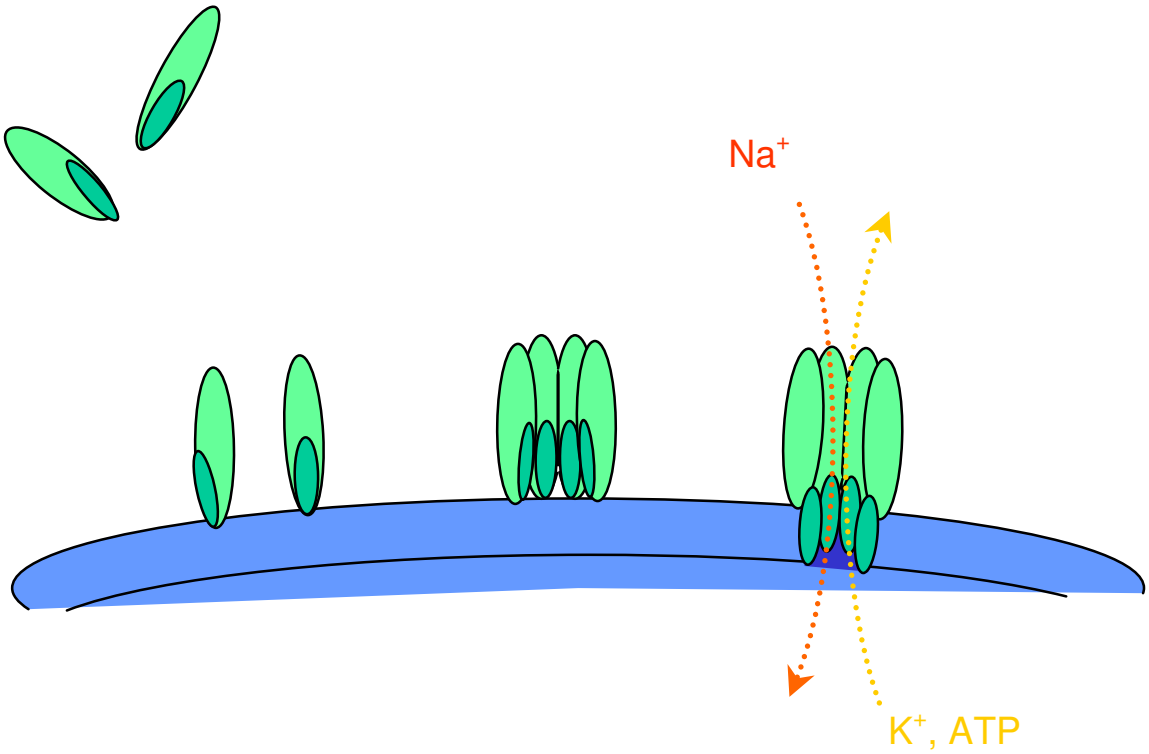

Figure 1.4: action of pore-forming toxins, from their water soluble to membrane inserted pore form.

Pore formation causes osmotic imbalance, which subsequently leads to cell swelling, lysis and death (*12*). It has emerged as a major and widespread mechanism for cell destruction in bacteria, plants, fungi, insects and animals (*13*).

Although most of these proteins are virulence factors, they are also used by cell biologists as tools for controlled permeabilization of cell membranes. In this application, they are usually superior to other membrane-permeabilizing agents such as digitonin or saponin, since the effects of the latter are normally difficult to predict, control or monitor (*14*). Detergents such as digitonin and saponin can only be applied in a narrow range of time and concentrations (*15*) and their use harbors the hazards of incurring direct damage to the secretory vesicles and or compromising other cellular functions (*16*).

Pore-forming toxins can also be designed to be expressed and exert their lethal effects on cancer cells. For example, Yang *et al*., investigated the effects of streptolysin O (SLO) on 293T cancer cells. They found that SLO attacks membranes and does not require any assistance from cellular proteins for its lethal attack, so there is little chance of the cell acquiring resistance by changing the expression levels of cellular proteins (*17*).

Other beneficial use of pore-forming toxins is in the control of pests. There are growing public concerns regarding the use of chemical insecticides. This has led to the extensive use of environment-friendly alternatives, of which the *Bacillus thuringiensis* δ-endotoxins are the main choice of the insect bio-control market (*18*). These toxins are highly specific to their insects, are innocuous to humans, vertebrates and plants and are completely biodegradable. Therefore, *Bacillus thuringiensis* is a viable alternative for the control of insect pests in agriculture and of important human disease vectors (*18*), (*19*).

1.3 Structural Classification of Pore-Forming Toxins

Bacterial pore-forming toxins (PFTs) can be broadly classified into two groups: Those that interact with the membrane through α helices, and those that utilize mostly β sheet structures such as β barrels (*11*). While the β-sheet interacting bacterial toxins (β-PFTs for short) include α-hemolysin from *Staphylococus aureus* and aerolysin from *Aeromonas hydrophila,* the helical (or α-PFT) family includes *Bacillus thuringiensis* δ endotoxins, and bacteriocins such as colicin Ia of *Escherichia coli* (*20*), (*21*).

The *B. thuringiensis* δ endotoxins are agriculturally important insecticidal agents (*11*) as mentioned above, which are thought to act through oligomerization (*21*). Colicins

secreted by *Escherichia coli* are agents of bacterial 'warfare' that kill sensitive strains of *E. coli* (*11*).

The conformation of the pores formed by the CAMP factor toxin, the monomeric or oligomeric structure and the molecular mechanism of CAMP factor toxin interaction with and insertion into membranes are still unknown. Known, however, is the relatively high percentage of α-helical content - approximately 30% as determined from the CD spectrum (*9*). This analysis also indicates about 19% β-strands, 22% turns and 29% random coil in the CAMP protein (*9*).

1.4 Membrane Interactions of α- and β-PFTs

Pore-forming toxins bind, oligomerize, then insert into the lipid bilayer. Membrane insertion requires a conformational change that exposes one or more hydrophobic structures hidden in the water-soluble monomer. These hydrophobic residues then insert into the membrane, forming the active pore.

Most pore-forming toxins studied to date do not contain extended hydrophobic sequences. The membrane-inserting domains of β-PFTs such as *Staphylococcus aureus* α-toxin, perfringolysin O and other cholesterol-dependent cytolysins, and anthrax toxin protective antigen consist of amphipathic sequences that, upon toxin oligomerization, interact with each other and form a membrane-inserted β-barrel, which surrounds the lumen of the pore (*22*). In the β-barrel, the β-hairpins are arranged in such a way that their hydrophilic residues are oriented towards the lumen, while the intervening hydrophobic residues face the membrane lipids (*22*), (*23*).

α-PFTs such as the pore-forming colicins and diphtheria toxin on the other hand contain hydrophobic and amphipathic α-helices long enough to span a lipid membrane (*22*). The hydrophobic α-helices are thereby buried within the toxin as long as it is in its water-soluble form (*22*). However, on the target membrane, partial unfolding of the toxin leads to a change in toxin conformation and insertion of the hydrophobic (and likely of amphipathic) α-helices as α-helical hairpins into the membrane, resulting in the generation of a transmembrane pore (*22*).

1.5 Alpha Pore Forming Toxins

The δ-endotoxins from *Bacillus thuringiensis* (B.t.) are insecticidal proteins that kill by forming pores in the epithelial cell membrane of some insect midgut (*24*). These toxins form crystalline parasporal inclusions and are ingested by insects, subsequently dissolving under the alkaline and reducing conditions in the midgut, whereupon cleavage by the gut proteases converts the protoxin to the active toxin (*24*). The activated toxin binds to the epithelial surface and causes pore formation in the cell membrane (*24*). The subsequent osmotic swelling and cell lysis result in cessation of feeding and breach of the gut-haemocoel barrier, killing the insect through starvation and septicaemia (*24*).

The δ-endotoxins form two multigenic families, *cry* and *cyt* (*25*). Members of the *cry* family are specifically toxic to insects in the three orders of *Lepidoptera, Diptera* and *Coleoptera,* due to their requirement for specific binding proteins (receptors) that are present on the midgut epithelial cell membranes (*26*). On the other hand, the *cyt* δ-endotoxins are specifically lethal to the larvae of *Diptera* insects (*27*). including the *Anopheles* and *Simulium* species that function as vectors for malaria and river blindness,

respectively (*28*), (*29*), (*30*). Although the class of α-PFTs contains many major virulence factors, the pore structures and even oligomeric stoichiometries of members of this family are still poorly characterized. This is because the oligomers aren't stable, thus, can't be extracted from membranes and characterized.

1.6 β-Pore-Forming Toxins

In contrast, the insertion pathways and pore structures of β-PFTs are much better understood. Like α-PFTs, β-PFTs are released as soluble monomers. β-PFTs oligomerize before forming active pores. The final insertion step often requires significant rearrangement of part of the structure, so that subunits can donate β-strands to form a trans-membrane β-barrel. For example, the pores formed by several *Staphylococcus aureus* toxins are well characterized. This applies to α-hemolysin (α-HL), which forms heptameric pores (figure 1.4 A), and to the leukocidins, which form hetero-octamers of LukF and LukS subunits (*31*) (figure 1.4 B, C).

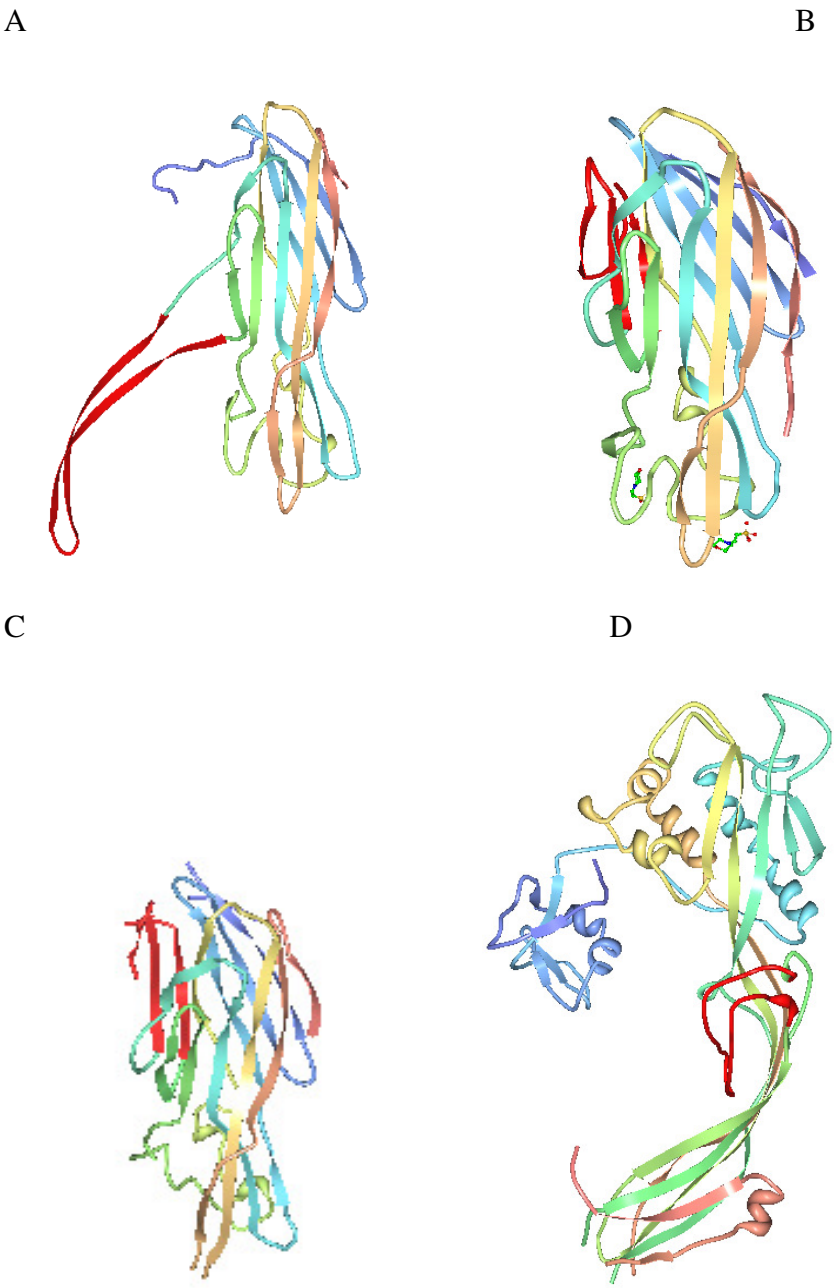

Figure 1.5: Structures of β-pore forming toxins. (A) α-HL subunit in the pore state, (B) LukF monomer, (C) LukS monomer, (D) aerolysin monomer. The regions that form the β -hairpins that insert into the membrane are coloured in red (*31*).

Most of the β-PFT such as aerolysin from *Aeromonas hydrophila* and α-HL oligomerize into a non-lytic pre-pore (a state where the toxin has oligomerized without its

trans-membrane domain inserted into the membrane) state on the membrane surface prior to insertion. After this step, insertion occurs, leading to the pore form. This pre-pore state is a common feature of other β-PFTs and has been trapped with suitably engineered disulfide bonds in *Staphylococcal* α-hemolysin (*32*). The conformational changes that occur during membrane insertion have been identified by comparing the monomeric structures from the bi-component leukocidin system with the pore state of α-HL (*33*). The hemolysin subunit has three domains – the cap, rim and stem domains - with mainly β-structure. In the water-soluble state, the stem domain is folded against the monomer core (*34*). To form the distinctive mushroom shape of the pore, the stem domains flip out and transform into β-hairpins to form a perfect trans-membrane β-barrel (*23*) figure 1.5 A, B).

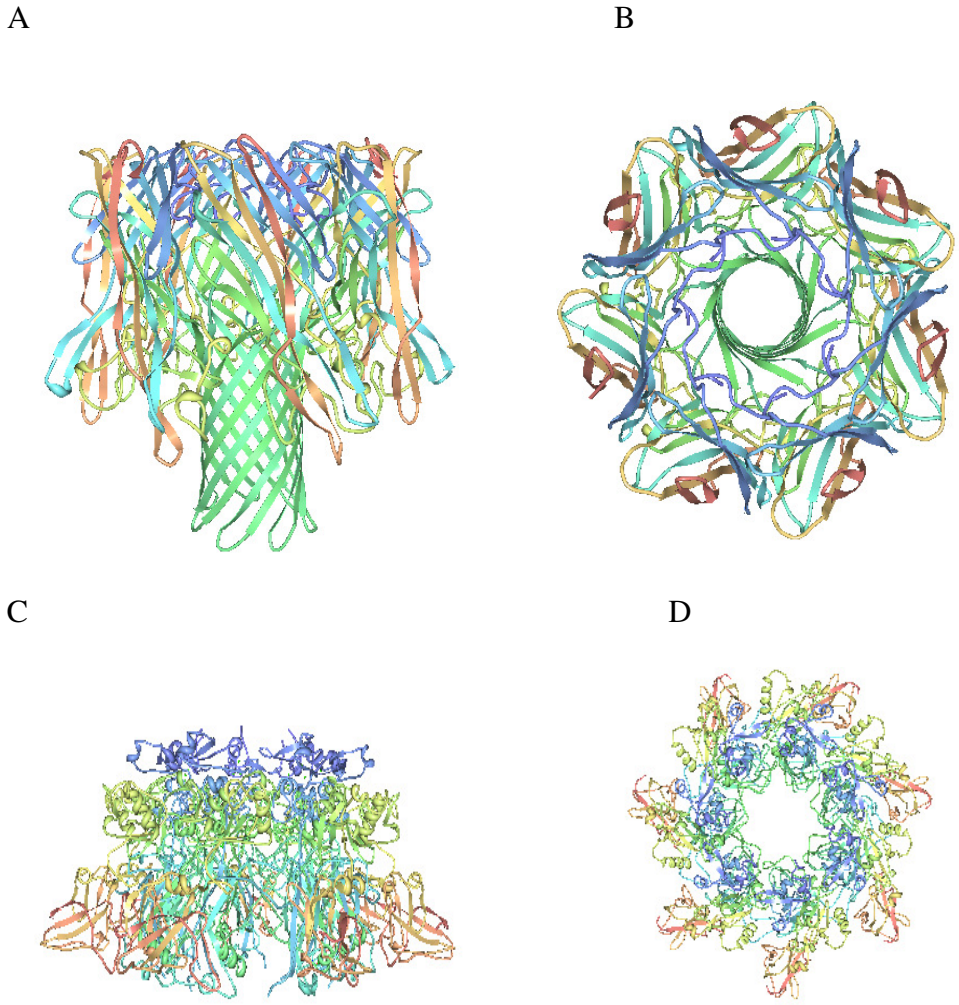

Figure 1.6: Oligomeric toxin structures. The α-HL pore viewed (A) from the side and (B) from the membrane. The β-barrel is formed from the β-hairpins. The hairpin-forming loop of anthrax protective antigen packs between subunits in the pre-pore state, as shown (C) from the side and (D) from the membrane (*31*).

Other well-characterized β-PFTs include aerolysin from *Aeromonas hydrophila* (figure 1.4 D), and the cholesterol-binding toxins (CBTs) produced by various gram-positive bacterial genera (*11*). CBTs contrast strongly with these other toxins in forming large ring- and arc-shaped oligomers with up to 50 subunits (*11*).

Structurally and functionally related CBTs (also know as thiol-activated toxins and cholesterol-dependent cytolysins) have been identified in five bacterial genera: *Streptococcus, Listeria, Bacillus, Clostridium*, and *Arcanobacterium* (*11*). A number of reviews have appeared on CBTs, including those by Gilbert (*11*), Alouf and Geoffroy (*22*) and Tweten (*35*).

The prerequisite for a CBT to attack a membrane is the presence of cholesterol in the membrane (*11*). Solving the X-ray crystal structure of a CBT (perfringolysin) revealed that it has an elongated, four-domain structure (*11*). The N-terminal 75% of the molecule contains three domains, with the polypeptide chain passing backwards and forward between them; the fourth, C-terminal domain has an immunoglobulin type fold and is involved in membrane binding (*36*) (figure 1.6).

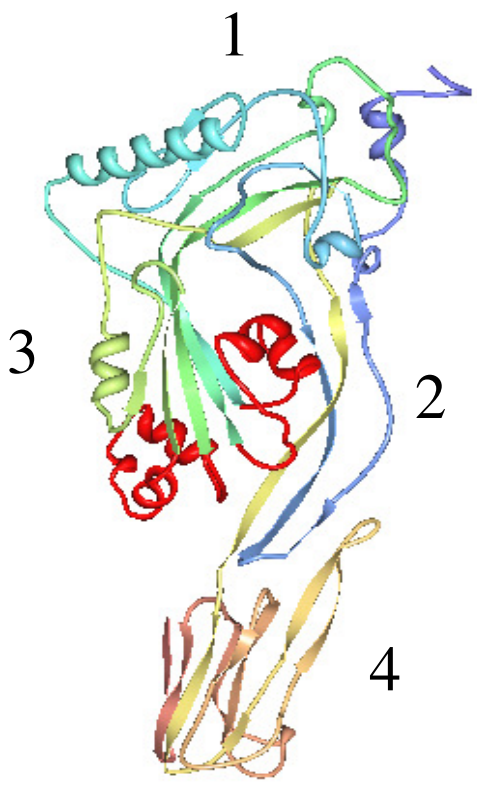

Figure 1.7: A view of the perfrinoglysin monomer solved by X-ray crystallography. The regions of domain 3 involved in pore formation are shown in red. The hook-shaped loop in domain 4 is involved in binding events.

1.7 "A-B" toxins

The principle of pore-formation also occurs in a class of toxins that are known as the "A-B toxins". In these toxins, trans-membrane pores function as transporters for enzymatic toxin moieties that, once delivered to the cytosol of the target cell, will cause cell death (*37*). Examples include cholera, ricin, diphtheria, tetanus, and anthrax toxins. Gill (*38*) named these "A-B toxins": the "A" portion is the active, enzymatic part of the toxin, and the "B" portion is the part of the toxin that binds to the cell membrane and translocates the A portion to the cytosol (*37*).

The B portion of these toxins make pores in planar lipid bilayers (*39*) and may adopt primarily beta transmembrane structure (anthrax, cholera toxins) or alpha transmembrane structure *(colicin E, Bt, diphtheria toxins).* Mutants that are defective in pore formation are also defective in poisoning cells (*40*). Diphtheria toxin (DT) secreted by *Corynebacterium diphtheriae* is a member of this A-B family of toxins. After proteolytic processing, the toxin consists of two polypeptide chains, A (21 kDa) and B (37 kDa), that are joined by a disulfide bond (*41*). The A chain is identical to the catalytic (C) domain of the protein, while the B chain consists of two domains, the receptor binding domain (R) and the transmembrane (T) domain (*41*). After entry into endosomes via receptor-mediated endocytosis, a conformational change triggered by the low pH of the endosomal lumen renders the toxin hydrophobic (*42*). This allows the toxin to penetrate the endosomal membrane and translocate its A chain into the cytosol. The final release of the A chain may follow reduction of the disulfide linking it to the T domain, perhaps with the aid of cytosolic proteins (*41*). Once in the cytosol, the A chain catalyzes the ADP-ribosylation of the diphthamide residue of elongation factor 2, which inhibits protein synthesis and leads to cell death (*43*) (*41*).

1.8 Membrane Interactions of α-Pore-Forming Toxins

The membrane interactions of the δ-endotoxin *Cry* will be discussed as a model for α pore forming toxins. The tertiary structures of six different three-domain *Cry* proteins, *Cry 1Aa, Cry2Aa, Cry 3Aa, Cry 3Bb, Cry 4Aa* and *Cry 4Ba* have been determined by X-ray crystallography (*19*), (*30*) (figure 1.7).

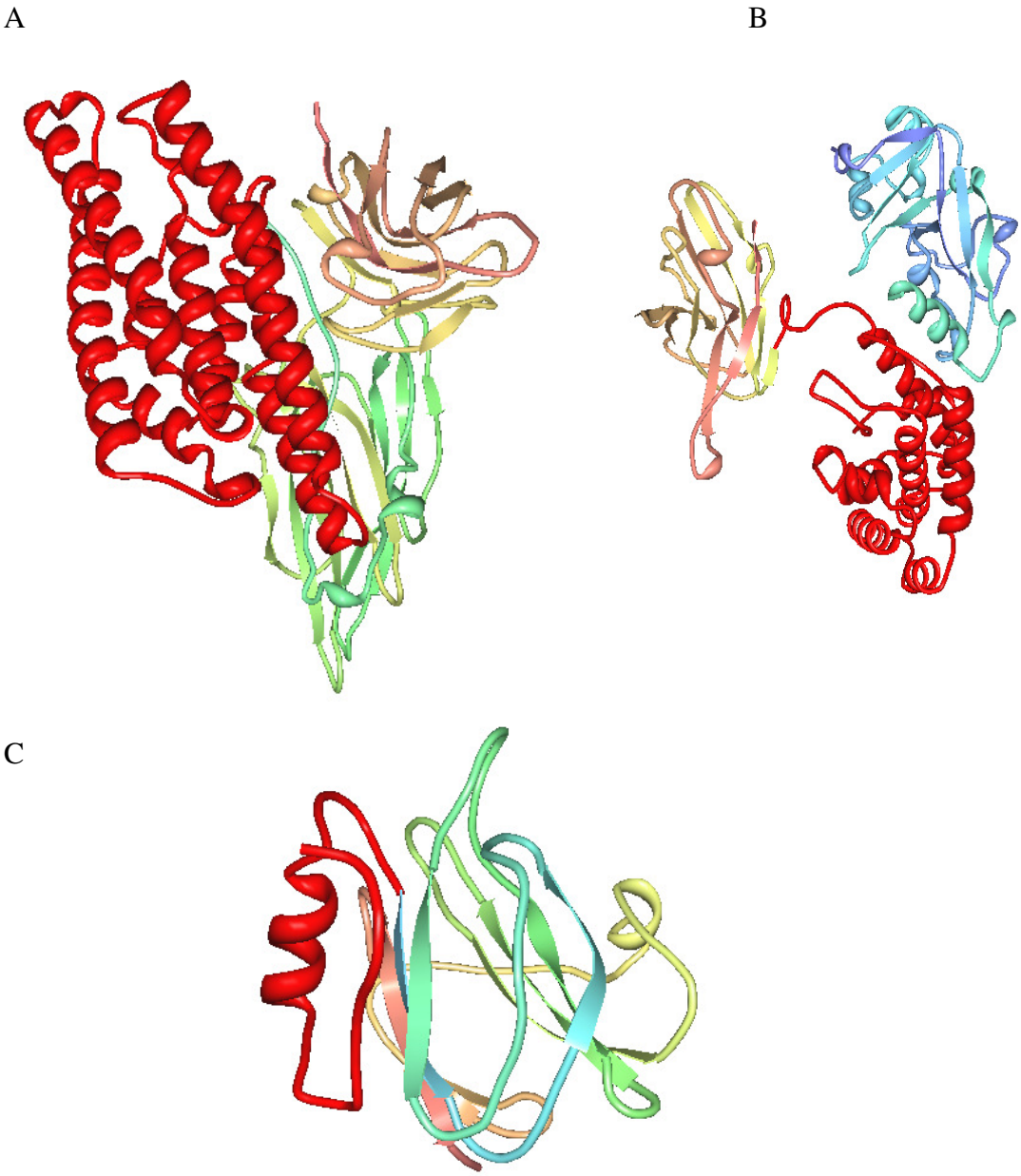

Figure 1.8: Structure of (A) the monomeric δ-endotoxin Cry 3Bb1 and (B) the Diphtheria toxin and (C) equinatoxin II. The membrane inserting regions are coloured in red.

All these structures display a high degree of similarity with a three-domain organization, suggesting a similar mode of action of the *Cry* three-domain protein family (*19*). The N-terminal domain (domain I) is a bundle of seven α-helices in which the central helix-α5 is hydrophobic and is encircled by six other amphipathic helices; and this helical domain is

responsible for membrane insertion and pore-formation (*19*) (figure 1.7). Domain II consists of three antiparallel β-sheets with exposed loop regions, and domain III is a β-sandwich (*30*), (*19*). Exposed regions in domains II and III are involved in receptor binding (*19*). Domain I shares structural similarities with other PFTs like colicin Ia and N and diphtheria toxin (figure 1.7), supporting the role of this domain in pore-formation (*19*). In the case of domain II, structural similarities with several carbohydrate-binding proteins like vitellin, lectins (class of carbohydrate-binding proteins), jacalin, and lectin Mpa have been reported (*44*). Domain III shares structural similarities with other carbohydrate-binding proteins and these similarities suggest that carbohydrate moieties could have an important role in the mode of action of three-domain *Cry* toxins (*19*). Interestingly, in the nematode *Caenorhabditis elegans,* mutations in *bree* genes involved in the synthesis of certain glycolipids lead to *Cry5* resistance, suggesting that glycolipids may function as receptor molecules of *Cry5* (*45*).

So far we've only been discussing pore forming proteins in the form of bacterial toxins; however, there also exist non bacterial pore-forming toxins such as the eukaryotic pore-forming toxin equinatoxin II from sea anemones, a representative of actinoporins (*46*) (figure 1.7). The membrane topology of this α-helix pore forming toxin and others such as diphtheria toxin, have been studied using different spectroscopic assays. These assays include cysteine scanning mutagenesis where BODIPY labeled with streptavidin was used to assay the accessibility of biotin attached to residues on diphtheria toxin (*47*) and IANBD labeling followed by hydrophilic quenching to study the N-terminus of equinatoxin (*46*). In the case of diphtheria toxin, the T domain has been observed to exist in two distinct conformations, shallowly and deeply inserted states (*48*). Just like

the diphtheria toxin, Equinatoxin II also shows these two states (*46*). Upon membrane insertion, variations in the behaviour of these toxins were detected every 3-4 amino acid residues (*46*) suggesting an alpha helical conformation.

1.9 Membrane Insertion Pattern of β-Pore-Forming Toxins

To determine directly how a particular residue interacts with cell membranes in membrane-bound PFT oligomers, that residue is replaced by a cysteine residue and covalently modified or bound to an environmentally sensitive fluorophore (*49*). This approach requires an otherwise cysteine-free protein. The spectral properties of the fluorescent label are then determined before and after it is bound to the membrane. N,N-dimethyl-N-(iodoacetyl)-N-(7-nitrobenz-2-oxa-1,3-diazolyl)-ethylenediamine (IANBD) has been the fluorophore of choice for many studies, because its emission intensity and lifetime both increase substantially upon moving from an aqueous solvent into the hydrophobic interior of the bilayer (*50*).

As seen in figure 1.8, if the toxin polypeptide spans the membrane in a β-sheet conformation, as does Perfringolysin O (PFO) from *Clostridium perfringens*, (*50*), then one would expect the environment of residues along the membrane-bound polypeptide to alternate between aqueous (facing the pore) and nonpolar (facing the core of the bilayer).

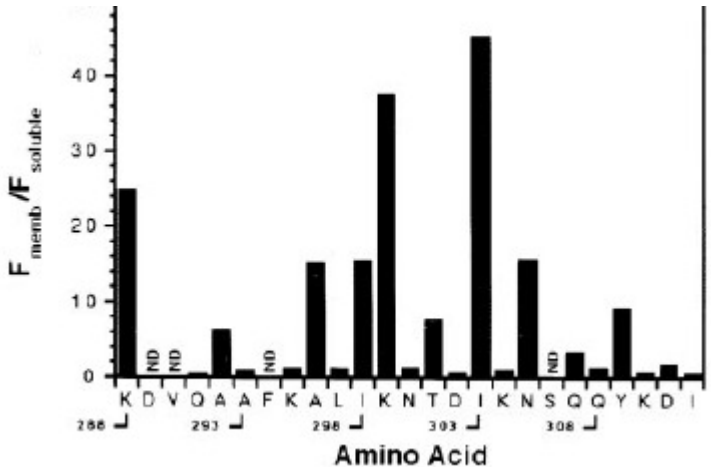

Figure 1.9: Membrane Binding-Dependent Fluorescence Changes of NBD Probes Located at Sites within TMH2. The emission intensity of a NBD-labeled PFO mutant was determined at 25 °C (Fsoluble) and then liposomes were added and incubated (37 °C, 10 min) before the emission intensity of the membrane-bound PFO was measured at 25 °C (Fmemb). The ratio of these two values indicate the extent of change of NBD environment upon binding to the membrane (a high ratio occurs when NBD moves from an aqueous to a nonpolar milieu) (*49*).

Alternatively, if the PFO inserts into the bilayer as an amphipathic α-helix, as proposed for SLO (*50*) then the periodicity of residues facing the aqueous pore or the nonpolar bilayer should conform to a helical wheel analysis of the residues in the α-helix (*50*).

When these membrane-permeabilizing toxins interact with membranes, a portion of the toxin/protein polypeptide will span the bilayer and form the interface between the aqueous channel and the non-polar core of the bilayer, in turn, forming pores. Structures of these membrane permeabilizing toxins are usually used to predict the transmembrane domains and then confirmed using techniques such as cysteine scanning mutagenesis and site-specific fluorescent labeling.

1.10 Modification of Cysteine

Chemical modification of amino acids is very important for the attachment of external probes such as fluorophores, to study the behaviour of proteins (*50*). Amino acids with amine, sulfhydryl, imidazol and carboxyl groups can all be covalently and selectively modified (*51*). Lysine residues can be selectively derivatized by a number of reagents, such as succinic anhydride and N-hydroxysuccinimide derivatives. However, the high frequency of occurrence of lysine residues in proteins makes it unfeasible to selectively modify a single residue. Although the histidyl side chain can react with halides and diethyl-pyrocarbonate, histidine residues are often critical for the biological activities of proteins and thus it is impractical to modify them (*51*).

Due to its relatively rare occurrence and possession of the strongest nucleophilicity among all standard amino acids, cysteine is the most convenient target for specific modification with various reagents (*52*). Site-directed mutagenesis makes it possible to place cysteine residues at defined positions in protein, and subsequently modify them with fluorescent probes. This is done for each amino acid residue in a region of interest in a strategy known as 'cysteine scanning mutagenesis'. This procedure has enabled mapping the topology of membrane proteins and the secondary structure of membrane-spanning regions in membrane proteins (*52*). Also, labelling cysteine mutants with reagents of different sizes and charges may result in a functionally altered protein, which will provide valuable information on its mechanism of action. As shown in figure 1.9, the sulfhydryl group of cysteine reacts with alkylating reagents such as haloacetamides and maleimides to form chemically stable products.

Iodoacetamide derivatives are the most commonly used reagents for attaching structural probes to cysteine residues. Examples of such reagents are N, N'-dimethyl-N-(iodoacetyl)-N'-(7-nitrobenz-2-oxa-1,3-diazol-4-yl)ethylenediamine (IANBD amide), N-iodoacetyl-N-(5-sulfo-1-naphthyl)ethylenediamine (1,5-IAEDANS), and 5-iodoacetamido-fluorescein. Iodoacetate esters also are occasionally used for introducing structural probes and preparing bio-conjugates. Examples include IANBD ester, and iodoacetate biotin derivatives.

Maleimide reacts rapidly with excellent specificity with cysteines in proteins. The reaction of N-ethylmaleimide with sulfhydryl groups can be monitored quantitatively by spectrophotometry (*52*). N-Ethylmaleimide has a maximum absorbance at 305 nm. Upon formation of the cysteine-maleimide adduct, the absorbance decreases in proportion to the extent of reaction. Maleimides hydrolyze in aqueous solution to non-reactive maleamic acids; in fact, the competition between cysteine modification and maleimide hydrolysis can be a serious problem at pH above 8 (*51*). There is a large collection of fluorescent labeling reagents that contain maleimide as the reactive group.

A

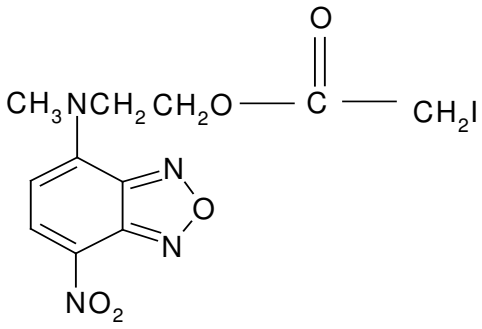

IANBD
MW 406.14

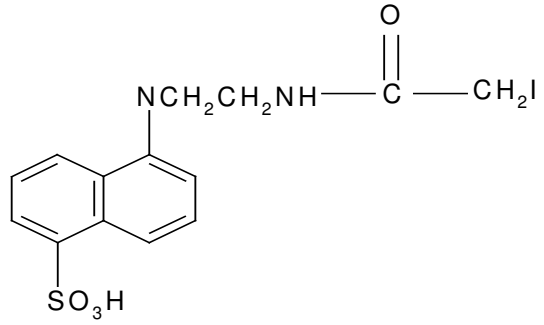

IAEDANS
MW 434.25

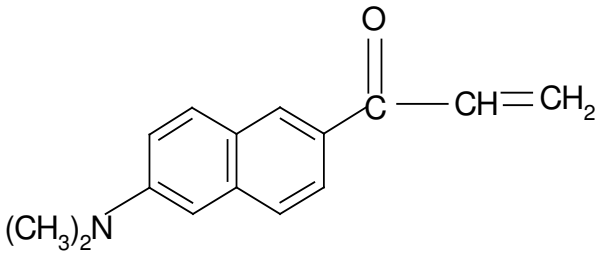

Acrylodan
MW 225.29

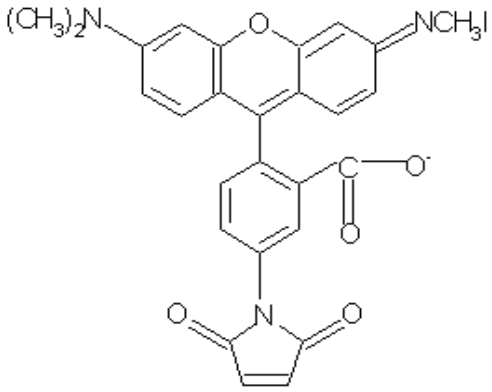

Fluorescein Maleimide
MW 485.51

B

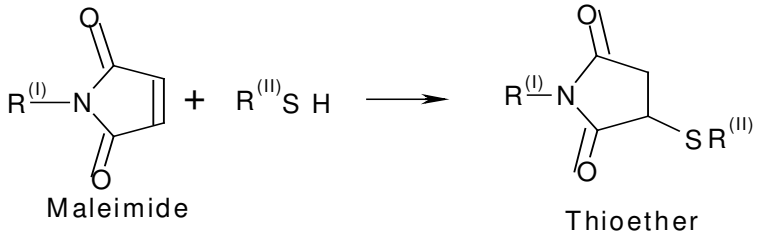

Maleimide

Thioether

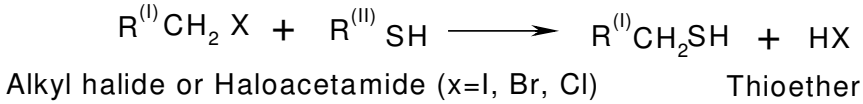

Alkyl halide or Haloacetamide (x=I, Br, Cl)

Thioether

Figure 1.10: A, Structures of some of the dyes used in cysteine scanning mutagenesis. B, the reaction occurring between the sulfhydryl groups of the protein and the modification reagents.

Insights regarding the structure of the pore-forming domain of CAMP factor within the membrane could significantly advance understanding of the mode of action of this toxin. Since CAMP factor is not homologous to any other toxin, its functional properties cannot be predicted based on similarities, so it is justified to study it experimentally.

Therefore, a hydropathy analysis of the toxin was performed by a previous MSc. student, Shanshan Liu, which provided a hydropathy plot of *S. agalactiae's* CAMP factor, identifying a hydrophobic region from amino acid T90 to V115. Using cysteine scanning mutagenesis and site specific labeling of mutants S101, G110, I111, T112, K113, and V115, she showed that these residues contact the membrane upon toxin binding and oligomerization on sphingomyelinase treated sheep red blood cells. In this study, mutants between residues T90 and V115 excluding those mentioned above were studied using cysteine scanning mutagenesis and site specific fluorescent labeling. Spectroscopic and lifetime analysis of these labeled mutants in solution and on membranes indicate that this region, T90 to V115, inserts into the membrane, and that residues N104 to F109 insert into the membrane with a β-sheet conformation.

2.0 Experimental Procedures

2.1 Reagents

Glutathione-agarose resin, glutathione, DL-dithiothreitol (DTT), aminobenzylpenicillin (Ampicillin), thrombin from human plasma, sphingomyelin phosphodiesterase (Sphingomyelinase) and bovine serum albumin (BSA) were purchased from Sigma-Aldrich (Oakville, ON). The BL 21 (DE3) strain of *Escherichia coli* was from Novagen (Madison, WI). The XL1 blue strain of *Escherichia coli* was attained from Clontech (Palo Alto, CA). pGEX-KG vector was a gift from Jingya Li (National Centre for Drug Screening, Shanghai, China). PWO DNA polymerase enzyme and deoxynucleoside triphosphates (dNTPs) were purchased from Roche (Mississauga, ON). Isopropyl β-thiogalactoside (IPTG), ethylene diaminotetraacetic acid (EDTA) and Triton X-100 were received from Bioshop (Burlington, ON). Restriction endonucleases *Bgl*II, *Spe*I, *Ssp*I, *Hind*III, *Eco*RV, *Sal*I, *Sna*BI, *Sty*I, *Mun*I, *Pvu*II, *Alw*21I, *Bciv*I, *Alw*NI, *Sca*I, *Bsp*1407I, *Pma*CI were from MBI Fermentas, as were the DNA marker and protein marker (Burlington, ON). PD-10 desalting columns were purchased from Amersham Biosciences (Baie D'Urfe, QC) and P-6DG desalting gel from BIO-RAD. Ethylenediamine (IANBD amide), Aamplexred cholesterol assay kit and sheep red blood cell were obtained from Cedarlane (Hornby, ON). β-Mercaptoethanol and dimethyformamide (DMF) were from EM SCIENCE (Gibbstown, NJ) and dimethyl sulphoxide (DMSO) from CALEDON. Plasmid DNA was prepared using QIAprep Spin Miniprep Kit from Qiagen (Mississauga, ON). PlUltrapure MiliQ water was used in all reactions.

2.2 Plasmids and Bacterial Strains

The plasmid pGEX-KG (61) containing the coding sequence of CAMP factor wild type and $CAMP^{M21L,M107L}$ double mutant were used. The $CAMP^{M21L,M107L}$ double mutant is active and for the purpose of this study equivalent to wild type CAMP factor. The coding sequence of these plasmids derived from wild type CAMP factor, amplified from *Streptococcus agalactiae* genomic DNA and matched the published mature peptide sequence for CAMP factor (*53*). All the mutagenesis was done in XL1 Blue *E. coli.* Transformations were done in a BioRad cell pulser electroporation unit according to the manufacturer's instructions. Plasmids were purified using QIAprep Spin Miniprep Kit from Qiagen, according to the manufacturer's instructions. All the wild type and mutant CAMP factor was expressed through BL21 (DE3) *E. coli*.

2.3 Verification of Mutagenesis

Residues from positions 90 to 115 were substituted individually for cysteine previously in the Palmer lab using a recombination based PCR protocol (*54*). The PCR products were then transformed into competent XL-1 blue cells (Palo Alto, CA) and the now transformed cells plated on 100 μg/ml ampicillin agar plates and grown overnight at 37 °C. Single colonies on the plates were selected and grown in 10 ml LB (Luria-Bertani) (Bioshop) broth containing 100 μg/ml ampicillin. The cells were then harvested and their DNA (plasmid) extracted. The extracted plasmids were subsequently digested with restriction enzymes deliberately incorporated into the mutated plasmids for selection purposes. After successfully identifying all the mutants, the plasmids were then transformed into competent BL21 (DE3) cells using electroporation and plated on

ampicillin agar plates. The cells were then grown as before and the plasmids extracted using the QIAprep Spin Miniprep Kit Protocol (Qiagen). Extracted plasmids were then sent to MOBIX lab, McMaster University, for sequencing.

2.4 Preparation of Competent XL-1 blue Cells and their Transformation

Fresh overnight XL-1 blue cells were inoculated into LB broth for a 1:100 dilution and grown at 37 ^{o}C to an optical density (OD_{600}) of 0.4. The cells were then spun at 3000 rpm at 4 ^{o}C for 10 min after which the supernatant was decanted. A 1 mL LB and 1 mL 2 x TSS buffer were added to the cells and re-suspended gently on ice. The now competent XL-1 blue cells were then aliquoted and stored at -70 ^{o}C until use. To transform the cells, 1 μL of plasmid DNA was added to 100 μL of thawed competent cells and incubated on ice for 45 min. The cells were then heat shocked by placing the tubes in a 42 ^{o}C water bath for 45 sec. The cells were then plated immediately on 100 μg/ml ampicillin agar plates.

2.5 Preparation of Competent BL21 (DE3) Cells, and their transformation

A high efficiency electro-transformation procedure was used to transform *Escherichia coli* BL21(DE3) (Novagen Madison, WI) cells from which protein synthesis was induced. A 1L L-Broth was inoculated with 10 mL of fresh overnight BL21(DE3) cell culture. These cells were grown at 37 ^{o}C with vigorous shaking to an OD_{600} of 0.6. Cells were harvested by centrifuging at 4,000g for 15 min. The supernatant was then removed and the pellet re-suspended in a total of 1liter of ice cold 10% glycerol. Cells were then centrifuged as before, resuspended in 0.5, then 250 mL of 10% glycerol, centrifuged, then

re-suspended to a final volume of 4mL in ice cold 10% glycerol. The re-suspended competent cells were aliquoted and stored at -80 ^{o}C. To transform these competent cells, 40 µL of the competent cells were mixed with 0.5 µL of plasmid DNA, mixed well and incubated on ice for 1min. The *E. coli* pulser apparatus was set to 1.80 KV for a 0.1 cm cuvette. The mixture of cells and plamid DNA were transferred to a cold electroporation cuvette, and the suspension was shaken to the bottom. The cuvette was placed in a chilled safety chamber slide. The slide was pushed into the chamber and pulsed once for every sample. Immediately after pulsing, the cuvettes were removed from the chamber and their contents added to 1mL of SOC (2% Bacto tryptone, 0.5% Bacto yeast extract, 10 mM NaCl, 2.5 mM KCl, 10 mM $MgCl_2$, 10 mM Mg SO_4, 20 Mm glucose) medium to maximize the recovery of transformants. The re-suspended cells were incubated for 1 hour at 37 ^{o}C with vigorous shaking, 225 rpm. Transformed cells were selected by plating on ampicillin agar plates.

2.6 DNA Extraction

To a micro-centrifuge tube, 1.5 mL of fresh overnight, mutant plasmid DNA transformed X-L1 Blue cells were added (*55*) The cells were centrifuged at 10,000 g for 2 min and the supernatant aspirated. The pellet was re-suspended in 100µL of solution 1 (50 mM glucose, 25 mM tris-HCl, Ph 8.0, 10 mM EDTA) and vortexed for 2 min. The cells were incubated at room temperature for 5min for bacteria to be lysed and the DNA released. To these cells, 200 µL of solution II (0.2 M NaOH, 1% SDS) was added and mixed by inverting for 5 sec. Finally, 150 µL of solution III (5 M potassium acetate) was added and mixed by inverting for 20 sec. The contents of the tube were incubated on ice for 5

min for the plasmid DNA to be selectively renatured. Following incubation, the tube was centrifuged at 12,000 g for 5 min and the supernatant containing the DNA was removed and placed in a new tube. An equal volume of TE (10 mM Tris pH 7.5, 1 mM EDTA pH 8.0)-saturated phenol-chloroform was then added to the DNA sample. The DNA sample was vortexed vigorously for 20 sec followed by centrifugation at 15,000 g for 5 min to separate the phases. The aqueous layer (DNA) was removed and added to a new tube after which an equal volume of chloroform : isoamyl alcohol (in a 24 : 1 ratio) was added. The steps of washing with chloroform, vortexing and centrifuging were repeated. Finally, the DNA was ethanol precipitated by adding 1 mL of cold 100% ethanol, incubating on ice for 30 min, centrifuging at 15,000 g for 10 min and decanting the supernatant. The pellet was washed with 70% ethanol, dried and re-suspended in TE buffer (*56*). The extracted DNA was verified by running a 2 µL sample on a 1% agarose gel. To extract DNA for sequencing, the Q1Aprep Spin Miniprep Kit Protocol (QIAGEN) was used.

2.7 Protein Induction and Purification

Protein induction and purification were performed according to published procedures (*57*) with minor variations. An overnight 20 mL culture of BL21 (DE3) transformed cells was inoculated into 1 litre of 2XYT (liquid medium, 10 gram yeast extract, 16 gram tryptone, 5 gram NaCl in 1 litre) (100 µg/ml Ampicillin) and grown at 37 ^{o} with shaking (250 to 300 rpm), until an OD_{600} of 1 was reached. Before inducing protein synthesis with isopropyl-β-D-thiogalactopyranoside (IPTG) (BioShop Canada Inc), 20 µL sample was removed and added to a 40 µL 1X SDS-PAGE[h] (sodium dodecyl sulfate polyacrylamide gel electrophoresis) sample buffer. Protein synthesis was then induced by adding IPTG

to a final concentration of 1 mM. The culture was grown for another three hours, after which a second 20 µL sample was collected, and added to a 20 µL 1X SDS-PAGE sample buffer. The samples were heated at 95 ^{o}C for 5 min, loaded on a 12% SDS-PAGE gel, and run at 200 V to verify induction of the protein.

Growth of *E. coli*, induction of protein synthesis, purification and thrombin cleavage of the recombinant protein was done essentially as described (*55*) with these deviations: Glutathione-agarose beads with the fusion protein adsorbed were washed 10 times. First 4 washes were done by 10 mL volumes of PBST buffer (16 mM K2HPO4, 150 Mm NaCl, pH 7.2 1% triton X-100, 0.1% B-mercaptoethanol). The next 4 washes were with 10 mL each PBS buffer (16 mM K2HPO4, 150 Mm NaCl, pH 7.2, 0.1% β-Mercaptoethanol). Finally, the column was washed twice with Thrombin cleavage buffer (50 mM Tris (pH 8.0), 150 mM NaCl, 2.5 mM CaCl2, 2 mM DTT). Following the numerous washing steps, 10 µg of thrombin was added to the column and the GST beads resuspended and incubated for one hour. The purified protein was run on an SDS-PAGE gel to confirm the purity of the protein.

2.8 Gel Filtration

Gel filtration of solubilized CAMP factor protein was performed by passing the protein sample over a PD-10 (Amersham biosciences Baie D'Urfe QC) column (diameter: 16mm : length 25cm) or Bio-Gel P-6DG (Bio-Rad Laboratories) desalting gel. The column was equilibrated at room temperature with elution buffer (50 mM Tris pH 7.5,150mM NaCl, 1 mM EDTA). The CAMP protein was eluted with 3.5 mL of elution

buffer and collected in portions of 0.5 mL. Eluate was checked for the presence of protein using the Bradford method (Coomassie brilliant blue G-250) for protein assay.

2.9 Labeling of CAMP Factor Mutant Proteins with NBD

Following gel filtration (to remove any traces of β-mercaptoethanol or dithiothreitol (DTT) that might interfere with the labeling process) IANBD (NBD) (Cedarlane Hornby, ON) was added to a concentration that provided a 10-fold molar excess of reagent over the CAMP protein. After 2 hours of incubation at room temperature, the reaction was quenched by the addition of DTT to 5 mM and the mixture filtered as before to separate labeled protein from excess NBD. The fractions containing the NBD-labeled toxin were pooled, made 10% in glycerol, aliquoted, quick-frozen in liquid nitrogen, and stored at – 81 ^{o}C until they were used. Successful labeling and removal of excess dye was verified by illumination of the band, and also the absence of fluorescence at the dye-front respectively on UV-transilluminated SDS gel, data not shown.

2.10 Hemolysis Assay

The next step was to determine the effects of the cysteine substitutions and the addition of a bulky group such as the NBD on the activity of these mutants. To this end, four hundred microliters of pelleted sheep erythrocytes (Cedarlane) were washed four times in Tris buffer (10 mM Tris-HCl, 150 mM NaCl, pH 7.4) by centrifugation. The erythrocytes were then resuspended in Tris buffer to 1% (v/v) (*58*). The cells were incubated at room temperature for 10 min with 10 mM $MgCl_2$ and 50 milliunits/ml sphingomyelinase from *Staphylococcus aureus* (Sigma). Serial two-fold dilutions of

CAMP factor were prepared in a microtiter plate in the former buffer. Then, cell suspension was added to a final concentration of 0.5% or red blood cells in each well, and a starting toxin concentration of 3 μM. Hemolytic activity was measured by the decrease in turbidity (A_{650}) using a 96-well plate reader (Spectramax 190, Molecular Devices, Sunnyvale, CA). Hemolytic titration was performed for all NBD-labeled and unlabeled mutant CAMP factor proteins; in each assay, the activity of the $CAMP^{M21L,M107L}$ mutant was measured as a control.

2.11 Membrane Binding

Four hundred milliliter of Bovine red blood cells was washed three times with PBS buffer, centrifuging at 2000 g for 4 min. The red blood cells were then osmotically lysed by washing with lysis buffer (5 mM Na2HPO4, and 5 mM NaCl, pH 7) and centrifuging at 14000 g for 10 min. The pellet (red blood cell membranes) was re-suspended in 1 mL Tris buffer (50 mM tris pH 8, 150 mM NaCl) followed by the addition of 0.8 μL and 10 μL $MgCl_2$ (1M) and sphingomyelinase respectively. The mixture was incubated at room temperature for one hour after which it was spun and washed once to remove residual sphingomyelinase; the supernatant from both centrifugation steps were discarded. The sphingomyelinase treated red blood cells were then separated into 4, 250 μL portions, followed by the addition of the CAMP factor protein. The red blood cell membranes-CAMP factor mixture was incubated at room temperature for one hour to allow binding. Samples were then tested for membrane binding. Samples were then centrifuged at 14,000 g, supernatant collected, and washed once to remove unbound toxin. The fluorescence of both the washed samples and supernatants were taken.

2.12 Spectrofluorimetry

Emission spectra were recorded in a PTI Fluorescence Master System (excitation wavelength, 480 nm: emission wavelength 530 nm). For each labeled mutant, samples of monomeric and membrane-bound CAMP proteins were examined. After examining the membrane-protein samples, the samples were centrifuged and washed once to remove unbound toxin. Supernatant and membrane-protein pellet were saved and their fluorescence emissions examined. These extra steps were required to correct the fluorescence intensity of the membrane-bound toxin for incomplete toxin binding.

Corrections were done as follows:

$$FI_{membrane,\ corrected} = FI_{membrane\ pellet} / (FI_{monomer} - FI_{supernatant}) \quad [2]$$

The emissions from the membrane bound the monomer toxins were then compared to obtain the emission changes as a result of membrane binding.

2.13 Cholesterol Assay

To determine the lipid composition of the bovine red blood cell membranes, a cholesterol assay was run on the membranes using the Amplex Red Choesterol Assay Kit (Molecular Probes). Briefly, The membrane samples were diluted in 1 X Reaction Buffer (20 mL of 0.5 M potassium phosphate, pH 7.4, 0.25 M NaCl, 25 mM cholic acid, 0.5% Triton X-100). A positive control was prepared by diluting a 20 mM H_2O_2 working solution to 10 μM in 1 X Reaction Buffer. To separate microplate wells, 50 μL of the diluted membrane samples and the controls were added. The reaction was initiated by adding 50

μL of the Amplex Red reagent containing horseradish peroxidase (HRP), cholesterol oxidase, cholesterol esterase to each microplate well containing the samples and control. The reaction was then incubated for 30 min at 37 ^{o}C protected from light. The fluorescence was measured with the Plate Spectro Fluorimeter (Molecular Devices Corp, Spectra Max Gemini XS) fluorescence microplate reader with an excitation of 530 nm and emission at 590 nm. The lipid concentration was found to be 1 mg/ml.

2.14 Fluorescence Quenching with Hydrophobic Quenchers

After the fluorescence emission of the membrane-toxin sample was recorded, the samples were spun down to separate bound toxin from unbound. The supernatant from the centrifugation procedure was saved and its emission also recorded. The membrane-toxin pellet was then resuspended in Tris buffer and the fluorescence measured. Thereafter, the hydrophobic quencher, 5-doxyl-stearic acid was added to the membrane-toxin samples at increments of 0.05 μmol/mg lipid up to 0.25 μmol/mg lipid, taking the fluorescent reading after each addition. A control sample containing only the membranes was also treated as above, and the successive stages subtracted from the corresponding samples. The data obtained from the quenching experiments were used to construct Stern-Volmer plots, the slopes of which were evaluated to determine the relative efficiency of quenching. The same procedure was also used for the 16-doxyl stearic acid quenching investigations.

2.15 Time Resolved Fluorescence Measurements

Time-resolved fluorescence measurements were taken using the Fluo Time 100 Compact Fluorescence Lifetime Spectrometer using the diode laser light source LDH-P-C-470 (PicoQuant, Berlin, Germany). Samples of NBD-labeled CAMP factor derivatives without membranes were excited in 1 cm x 1 cm quartz cuvettes in 50 mM Tris buffer, 150 mM NaCl, pH 8. For samples containing membranes, the labeled toxin was added, incubated for 1 hour, and washed to remove any unbound toxin before obtaining the measurement. Experimental decays were fit with three exponentials; allowing for a fourth component did not improve the goodness of the fits. From these three components, an average lifetime for each sample was calculated using equation [1].

$$\langle \tau \rangle = \Sigma a_i \tau_i / \Sigma a_i \qquad [1]$$

Here, a_i represents the amplitude at time zero and τ_i the lifetimes of the *i*th component.

3.0 RESULTS

3.1 Construction of Mutants

With the exceptions of mutants S101C, G110C, I111C, T112C, K113C, and V115C, which were constructed by Shanshan Liu, all mutants discussed below were constructed as part of this work. All mutants were expressed as glutathione-S-transferase CAMP factor (GST-CAMP factor) fusion proteins. Mutants were confirmed by restriction analysis and DNA sequencing and expressed in *E. coli* BL21 (DE3) cells.

3.2 Purification of Mutants H95C to L114C

Transformed cells were grown in rich media and protein expression induced. Purification of protein was successful with all mutants but three; the three exceptions were Q94C, A103C and L114C. In the case of mutant A103C, no detectable protein synthesis was observed. This lack of protein synthesis could be the result of an additional substitution mutation, T97A, in the amino acid sequence. On the other hand, mutant L114C expresses the 52kDa fusion GST-CAMP factor protein when a sample of the induced culture is run on an SDS-PAGE gel. After lysing the cells, however, the protein is lost in the pellet during centrifugation, which means that it is aggregated and possibly misfolded. The purification procedure was repeated several times, each time changing parameters such as growing cells at lowered temperatures and keeping the harvested cells and cell lysate as close as possible to 4 °C. These alterations to the purification procedure did not result in making the protein soluble. As a result, L114C and A103C could not be purified and studied, and are not included in the data set generated. In

contrast, the primers of mutant Q94C still needs to be designed and thus also not included in the data set.

3.3 Production and IANBD Labeling of Cysteine Mutants

Mutants were labeled with the thiol-specific probe IANBD. No reaction between IANBD and wild type was detected. The extent of labeling was mutant-dependent and ranged from 20% (D106C) to 80% (F109C)**.** These mutants were then assayed for hemolytic activity and binding to sphingomyelinase treated sheep red blood cells. Table 3.1 shows a summary of the activities of the labeled and unlabeled mutants in comparison to the wild type toxin.

CAMP Mutants	Hemolytic Activity of NBD-Labeled Mutants Compared to Unlabeled Mutants	Hemolytic Activity of NBD-Labeled Mutants Compared to Wild-Type CAMP factor
L96C	Unchanged	Reduced by factor of 2
A97C	Increased by factor of 2	Unchanged
N98C	Increased by factor of 2	Decreased by factor of 2
K99C	Increased by factor of 4	Decreased by factor of 16
V100C	Increased by factor of 4	Increased by factor of 2
Q102C	Increased by factor of 4	Unchanged
N104C	Increased by factor of 8	Decreased by factor of 4
I105C	Increased by factor of 2	Unchanged
D106C	Increased by factor of 2	Decreased by factor of 4
L107C	Increased by factor of 2	Unchanged
G108C	Increased by factor of 2	Decreased by factor 2
F109C	Unchanged	Unchanged

Table 3.1: Hemolytic activity of NBD-labeled CAMP factor compared to the un-labeled cysteine mutants and the wild type protein.

With the exceptions of mutant K99C, Q102C, N104C and D106C, all labeled mutants had activities comparable to that of the wild type toxin. This hemolysis assay is meant as a control, to abolish any doubt of mutant activity. The activity of these labeled mutants therefore suggests same behaviour on membranes. Also, since the hemolysis assay tests limiting dilutions, it is not unlikely that even the mutants that perform sluggishly in the hemolysis assay react completely in the fluorescence assay since the fluorescence assays use higher concentrations of mutant toxins.

3.4 Changes in NBD Environment Detected by Emission Fluorescence and Lifetime Measurements

Emission spectra were obtained for each monomeric NBD-labeled mutant in solution and when bound to sheep ghost membranes pretreated with sphingomyelinase. In solution, λ_{max} from mutants H95C to F109C ranged from 531 (N104C) to 541 nm (F109C), indicating a relatively high degree of exposure of the NBD probe to the solvent (*46*). Mutant G108C however behaves differently; in solution, its emission maximum is at 526 nm, signifying a less polar environment.

Upon interaction with sheep red blood cell membranes treated with sphingomyelinase, all mutants exhibited an increased intensity and a blue shift in NBD fluorescence indicating the change in the polarity of the NBD environment. The mutant G108C retained its blue-shifted wavelength after membrane binding yet also exhibited an increase in NBD fluorescence, suggesting a more hydrophobic residence after membrane binding. Figure 3.1 shows example emission scans from mutants of adjacent residues, D106C and L107C in the monomeric and membrane-bound forms, showing the increase in intensity after membrane binding. The increase in intensity after membrane binding

was observed for all tested mutants though to different extents (appendix A). Figure 3.1C shows wavelength maxima of mutants from H95C to F109C. Residues H95C to F109C for which the wavelengths are shown, the λ_{max} were shifted to lower wavelengths by approximately 10 nm figure 3.1C. The values now range from 521 (N104C and F109C) to 534 nm (N98C). This increase in intensity and blue shifts of all tested mutants indicate a transition to a hydrophobic environment by the NBD dye attached to the mutants. Also apparent is a pattern in the wavelengths – notice the high and low blue shifts between N104C to F109C. The deeply inserted residues show a more reduced wavelength. Even more striking is the difference in wavelength between the membrane bound and monomeric mutants I105C, L107C and F109C. These mutants show about a 20 nm difference in wavelength between the membrane-bound and monomeric forms, and are more blue-shifted than the other mutants. This makes sense because the deeply inserted residues should be shielded more and thus exhibit higher blue shifts.

A

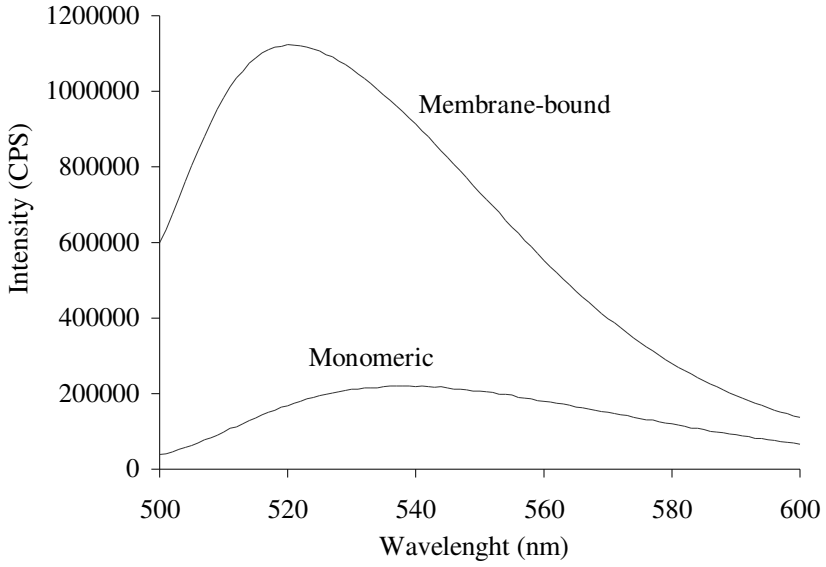
1200000
1000000
800000
600000
400000
200000
0
Intensity (CPS)
Membrane-bound
Monomeric
500
520
540
560
580
600
Wavelenght (nm)

B

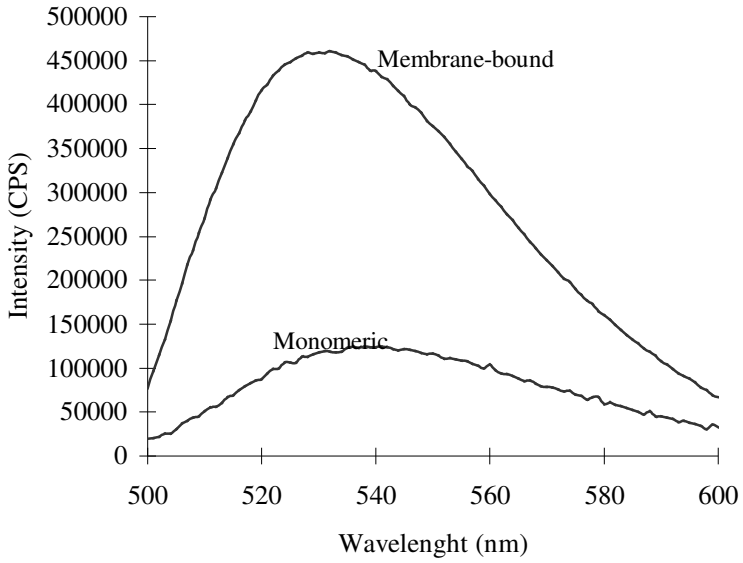
500000
450000
400000
350000
300000
250000
200000
150000
100000
50000
0
Intensity (CPS)
Membrane-bound
Monomeric
500
520
540
560
580
600
Wavelenght (nm)

C

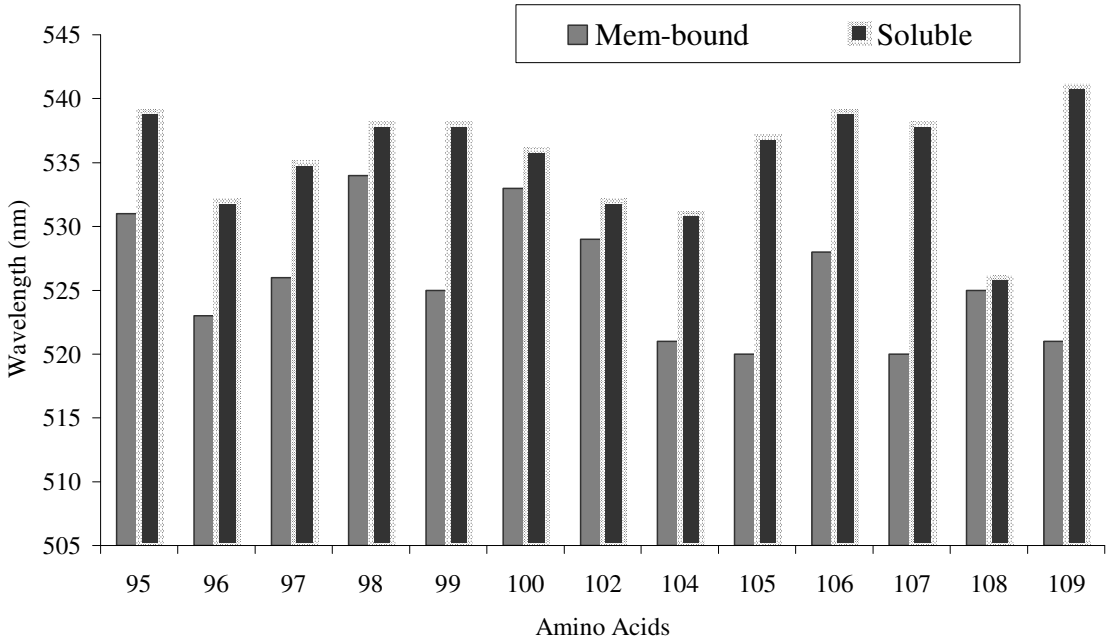

Figure 3.1: Fluorescence intensity and emission maxima of NBD attached to cysteine-substituted residues. Emission scans of the soluble monomeric and membrane-bound forms of NBD-CAMP factor L107C (A) and NBD-CAMP factor D106C (B) are shown. C, wavelength maxima of soluble and membrane-bound mutants H95C to F109C.

The combined fluorescence data for all residues within the region from T90C to V115C are summarized in figure 3.2 A.

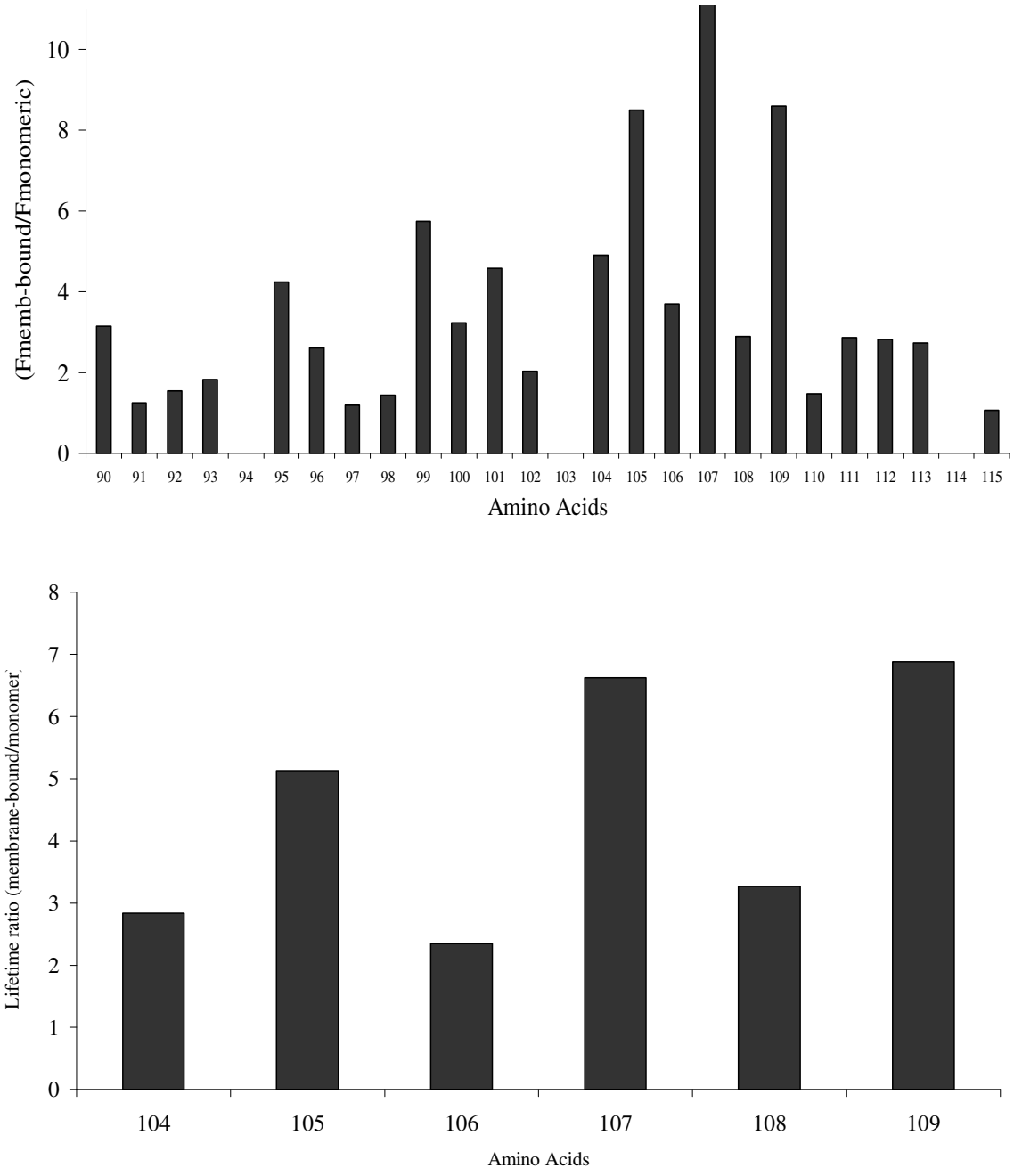

Figure 3.2: A, Relative changes in the NBD emission intensity upon membrane binding of mutants T90C to V115C. B, Ratios of the excited state lifetimes of membrane-bound and soluble, monomeric NBD labeled CAMP factor mutants from residues N104C to F109C.

The change in the emission intensity of NBD was determined from the ratio of the fluorescence in the membrane-bound ($F_{membrane}$) and soluble ($F_{soluble}$) states. The intensity of the membrane-bound toxin was corrected for incomplete toxin binding as described in the methods section. The increased intensity upon membrane binding observed with most mutants indicates movement of the dye into a more hydrophobic environment. Upon examination of figure 3.2A, specifically the region between residues N104C to F109C, one sees again an alternating pattern of low and high intensity changes**.** To further characterize the behaviour of these residues within this region, we measured the fluorescence lifetimes of the labeled mutants before and after membrane binding. The lifetime of the excited state is an intrinsic property of the probe and therefore is not affected by sample concentration and is independent of relative standards. In addition, while the signal observed in steady-state fluorescence is an average value and may obscure heterogeneity in the sample (*49*), lifetime analysis has the potential to reveal the fractions of dye molecules in different environments. If, on the other hand, the different signals observed in the steady-state spectra were truly characteristic of the protein and not caused by sample heterogeneity, a similar pattern should emerge from their lifetime measurements.

Time-resolved measurements are widely used in fluorescence spectroscopy, particularly for studies of biological macromolecules (*59*). This is because time-resolved data frequently contain more information than is available from the steady-state data (*59*). There are two methods of measuring time-resolved fluorescence: the time-domain and frequency domain.

For the purpose of this study, we will discuss the time-domain method. In this method, the sample is excited with a pulse of light. The width of the pulse is made as short as possible and is preferably much shorter than the decay time τ of the sample. The time-dependent intensity is measured following the excitation pulse, and the decay time τ is calculated from the slope of a plot of log $I(t)$ versus t.

Suppose a sample containing the fluorophore is excited with an infinitely sharp pulse of light. This results in an initial population (n_o) of fluorophores in the excited state. The excited-state population decays with a rate $\Gamma + k_n\Gamma$ according to

$$dn(t)/dt = -(\Gamma+k_{nr})\, n(t) \qquad [3]$$

Where $n(t)$ is the number of excited molecules at time t following excitation, Γ is the emissive rate, and k_{nr} is the non-radiative decay rate. Equation 3 states that both emission and non-radiative decay are random events, such that each excited fluorophore has the same probability of emitting or decaying non-radiatively in a given period of time.

In a fluorescence experiment we do not observe the number of excited molecules, but rather a fluorescence intensity, which is proportional to $n(t)$. Hence, Eq. [3] can also be written in terms of the time-dependent intensity $I(t)$. Integration of that form of Eq. [3] yields the expression for a single exponential decay

$$I(t) = I_0\, e^{-t/\tau} \qquad [4]$$

where I_0 is the intensity at time zero. The lifetime τ is the inverse of the total decay rate: $\tau = 1/(\Gamma + k_{nr})$.

In general, the inverse of the lifetime is the sum of the rates that depopulate the excited state. The fluorescence lifetime can be determined from the slope of a plot of log *I(t)* versus *t* (*59*). If there is one lifetime, we will expect a single exponential decay and a straight line in the semi-logarithmic plot; if there are multiple lifetimes, the semi-log plot will be convex, as shown in figure 3.3.

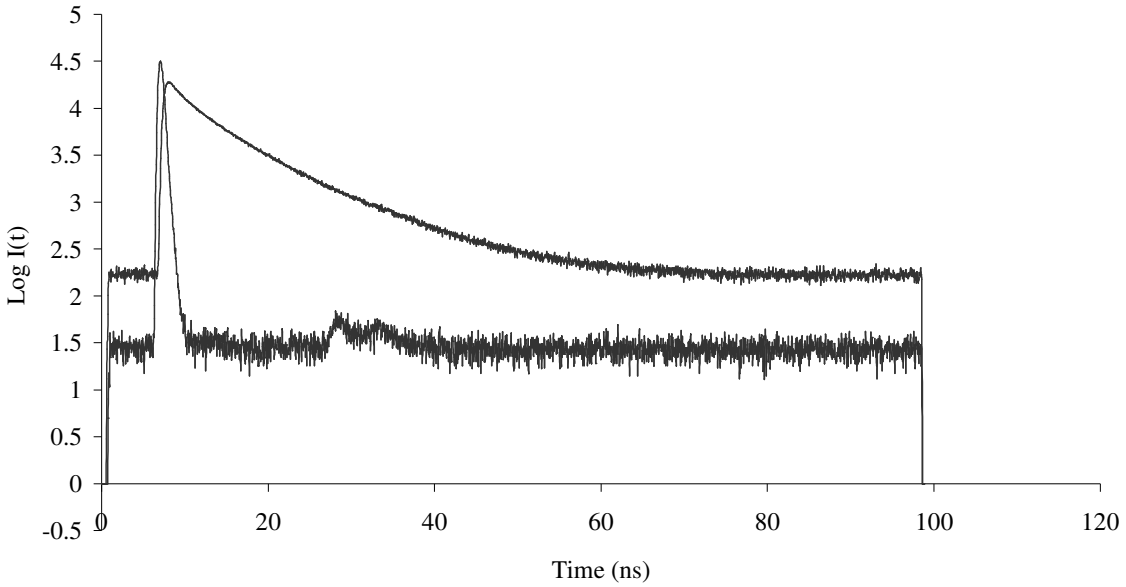

Figure 3.3: Intensity decay measurement of mutant L107C. Notice the curvature in the graph, indicative of a multi-exponential decay.

Time-resolved measurements were performed for mutants labeled at residues N104C to F109C. In every monomeric sample, the fluorescence lifetime data indicated the presence of three lifetime components table 3.2. The membrane-bound samples also display three different amplitudes with three different lifetimes: however, all lifetime

components of the membrane-bound samples are longer than those observed with the monomeric samples. These three different lifetimes are not likely related to any property of the protein or to heterogeneous probe environments because the free dye itself also shows three lifetimes. Therefore, the occurrence of multiple lifetimes is most likely a property of the dye.

	Free monomer		Membrane-bound	
	I_0	Lifetime (ns)	I_0	Lifetime (ns)
τ_1	2753	4.603	14523	10.053
τ_2	15012	1.252	14807	4.258
τ_3	64064	0.489	12240	0.954
$\tau_{average}$	81829	0.77	41570	5.3

Table 3.2: Fluorescence lifetime measurements of NBD-labeled monomeric and membrane-bound mutant L107C.

A weighted average lifetime was calculated from these three different amplitudes and lifetimes using equation [1]. From this average, we see the monomeric mutants having an average lifetime of about 1ns, and about 5ns after membrane binding, signifying the movement of the dye into a hydrophobic environment. When the ratios of the lifetimes between the membrane-bound and monomeric samples are taken, the same alternating pattern observed in the steady state and the blue shifts in wavelengths is apparent (figure 3.2 B). More importantly, the residues that exhibited the highest in blue shifts are those residues that show the highest change in intensity and lifetimes.

3.5 Residues from T90 to K113 Insert Into the Membrane

The location of the residues shown to enter a non-polar environment was confirmed by nitroxide quenching analysis. Nitroxides are efficient quenching agents of NBD as previously shown by Chattopadhyay (*60*) and, when attached to the fatty acyl chain of stearic acid, nitroxides can be introduced into natural membranes and will only quench fluorophores exposed to the bilayer core (*56*).

Fluorescence quenching refers to any process that decreases the fluorescence intensity of a sample (*59*). A variety of molecular interactions can result in quenching. These include excited-state reactions, molecular rearrangements, energy transfer, ground-state complex formation, and collisional or dynamic quenching (*59*). In the case of collisional quenching, the quencher must diffuse to the fluorophore during the lifetime of the excited state. Upon contact, the fluorophore returns to the ground state without emission of a photon (*59*). For dynamic quenching to occur, the fluorophore and quencher must be in contact. The requirement of molecular contact results in the numerous applications of quenching (*59*). For example, quenching measurements can reveal the accessibility of fluorophores to quenchers (*59*).

Collisional quenching of fluorescence is described by the Stern-Volmer equation

$$F_0/F - 1 = k_q \tau_0 [Q] = K_D [Q] \qquad [2]$$

In this equation, F_o and F are the fluorescence intensities in the absence and presence of quencher, respectively, k_q is the bimolecular quenching constant, τ_o is the lifetime of the fluorophore in the absence of quencher, and [Q] is the concentration of quencher.

Quenching data are usually presented as plots of $F_o/F-1$ versus [Q]. This is because $F_o/F-1$ is expected to be linearly dependent upon the concentration of quencher. A linear Stern-Volmer plot is generally indicative of a single class of fluorophores, all equally accessible to quencher. If two fluorophore populations are present, and one class is not accessible to quencher, then the Stern-Volmer plots deviate from linearity toward the x-axis (*59*). If the quenching is known to be dynamic, the Stern-Volmer constant (obtained as the slope of the plot) will be represented by K_D and be equal to $k_q\tau_o$. Otherwise, this constant will be denoted as K_{SV}.

3.5.1 *Quenching with 5-Doxyl Stearic Acid*-The characteristics of this quencher is that its nitroxide moiety is positioned close to the surface of the membrane and so any dye close to the surface of the membrane should be quenched (figure 3.4) (*61*).

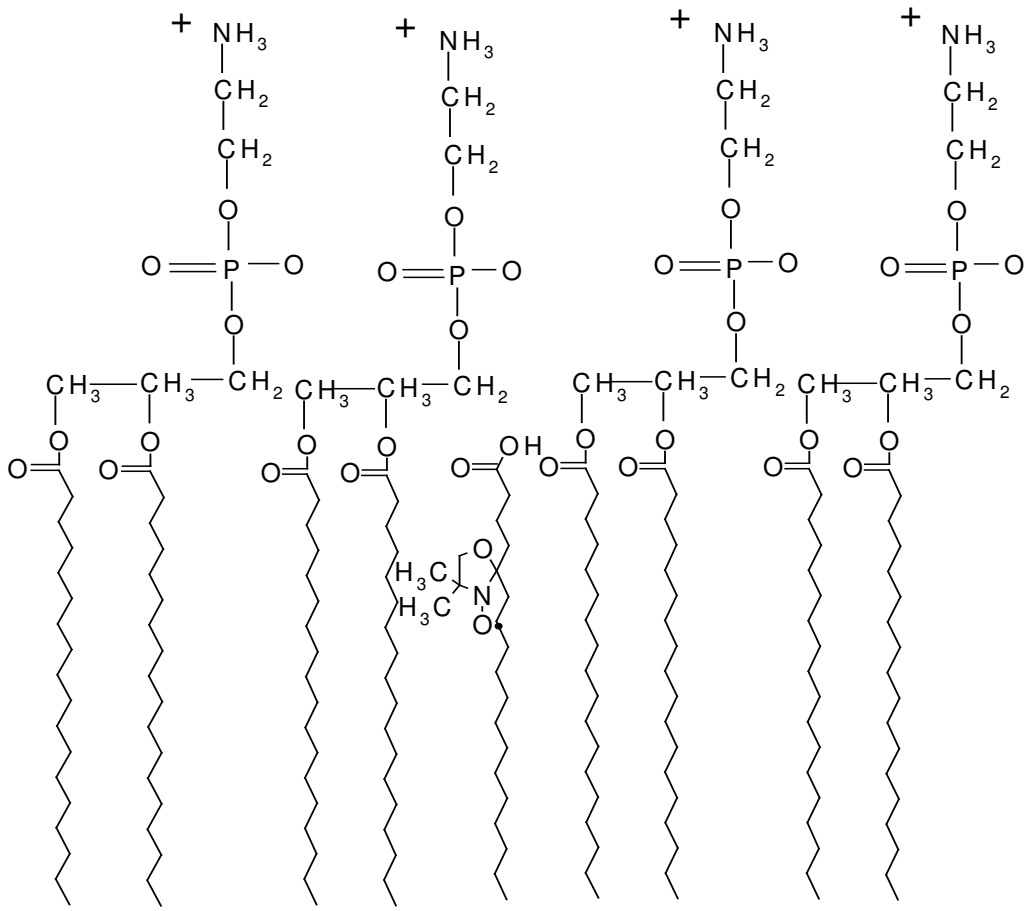

Figure 3.4: A diagram depicting 5-DSA within a phosphatidylcholine monolayer (which may be either the Trans or the Cis side of the membrane).

Quenching data for NBD dyes positioned adjacent to each other in CAMP factor are shown in figure 3.5 for the membrane-bound CAMP factor.

A

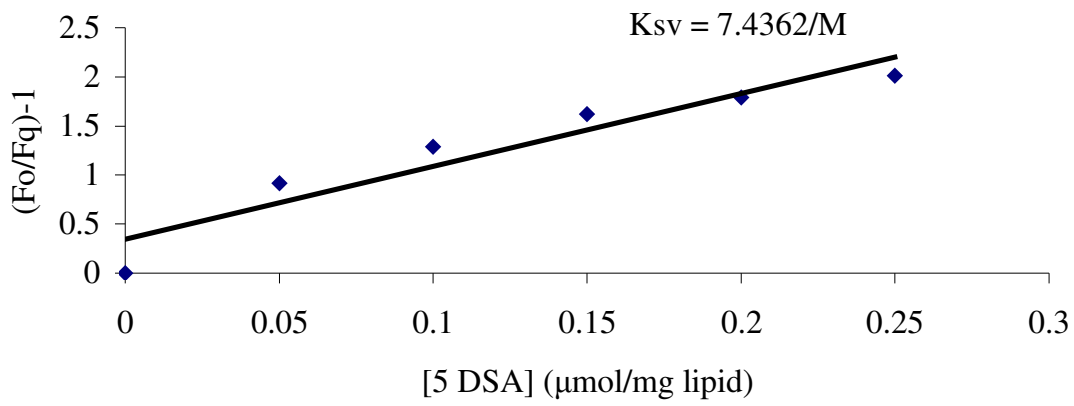
Ksv = 7.4362/M
(Fo/Fq)-1
2.5
2
1.5
1
0.5
0
0
0.05
0.1
0.15
0.2
0.25
0.3
[5 DSA] (µmol/mg lipid)

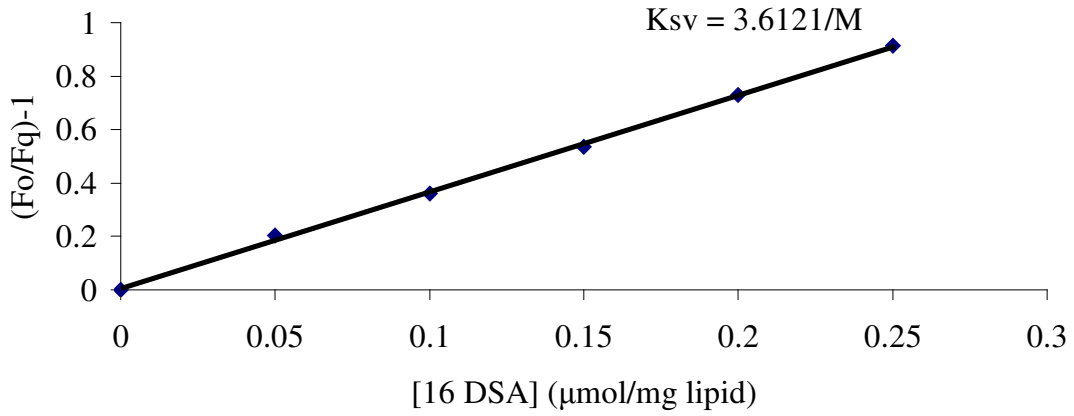
Ksv = 3.6121/M
(Fo/Fq)-1
1
0.8
0.6
0.4
0.2
0
0
0.05
0.1
0.15
0.2
0.25
0.3
[16 DSA] (µmol/mg lipid)

B

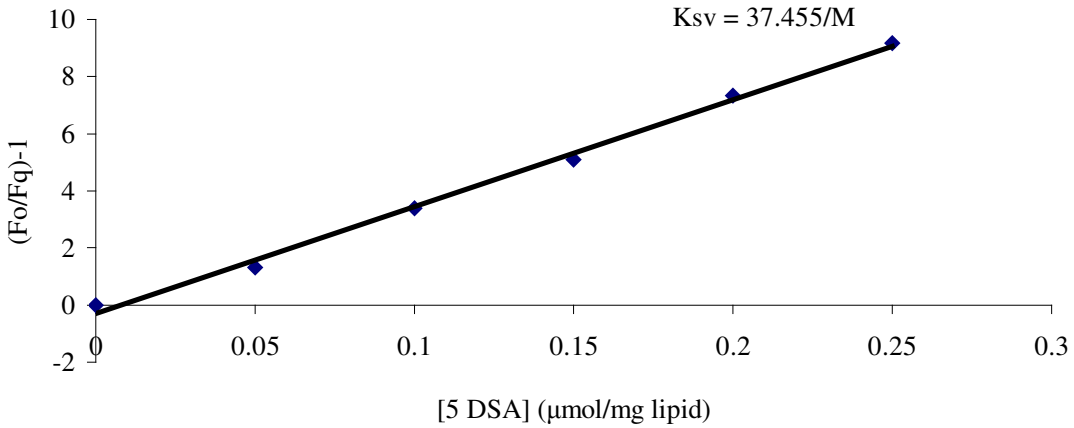
Ksv = 37.455/M
(Fo/Fq)-1
10
8
6
4
2
0
-2
0
0.05
0.1
0.15
0.2
0.25
0.3
[5 DSA] (µmol/mg lipid)

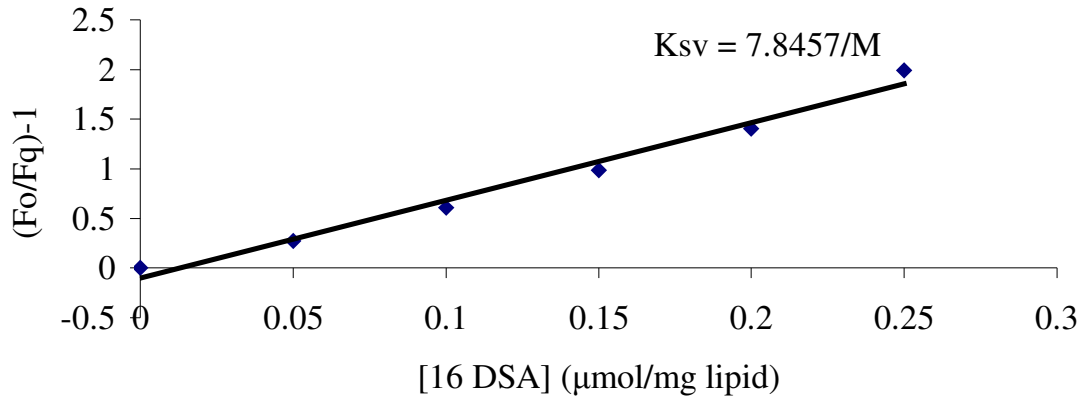

Figure 3.5: Stern-Volmer plots of mutants D106C and L107C quenched with 5 and 16-Doxyl Stearic Acid. Ksv represents the Stern-Volmer slope. The higher degree of quenching of both mutants by 5 Doxyl Stearic Acid is reminiscent of the higher Ksv values.

A linear Stern-Volmer plot as exhibited by most of these mutants is generally indicative of a single class of fluorophore, all equally accessible to quencher (*59*). In the Stern-Volmer plots, some of the mutants show deviations from linearity; this is most notable with mutant D106C. It needs to be determined whether or not these deviations are systematic. Figure 3.6 shows a summary of the pattern of quenching by 5-Doxyl Stearic Acid (5-DSA) as determined by their Stern-Volmer slopes.

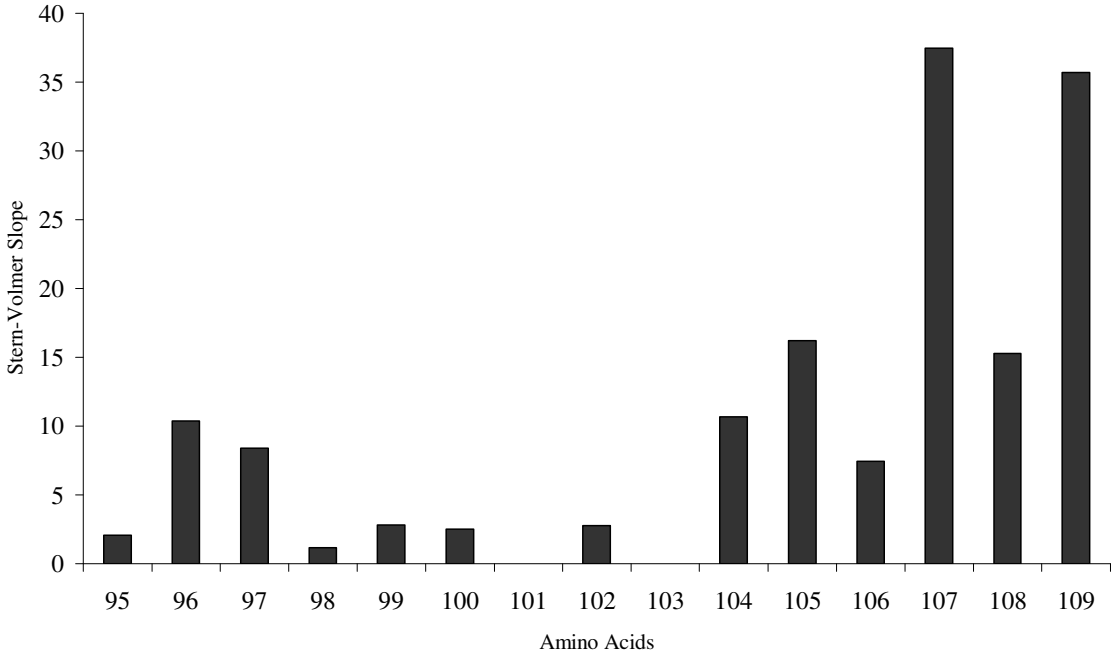

Figure 3.6: 5-Doxyl-stearic Acid Quenching pattern of NBD-labelled, membrane-bound mutants from residues H95C to F109C. Plot is generated from the slopes of Stern-Volmer plots. Notice the alternating pattern between residues N104C to F109C.

What we see in this figure is that there is quenching of all tested mutants as determined by their Stern-Volmer slopes, but the degree of quenching is dependent on the mutant. As with the lifetime and intensity change ratios, we again see the same alternating pattern of low and high quenching from residues N104C to F109C.

3.5.2 *Quenching with 16-Doxyl Stearic Acid*-So, membrane inserted residues of the region of CAMP factor under study are quenched by a superficially residing quencher such as 5 doxyl stearic acid, but what will the results be when a quencher buried deeper in the membrane is employed? When the protein inserts into the membrane, individual residues may reside deeply or shallowly in the membrane. So, by comparing the effectiveness of quenching by a superficially located quencher with a more deeply inserted one, we can get an idea about a residue's depth of insertion. We chose to

explore the quenching capabilities of 16-Doxyl Stearic acid on membrane-bound NBD-labeled CAMP factor.

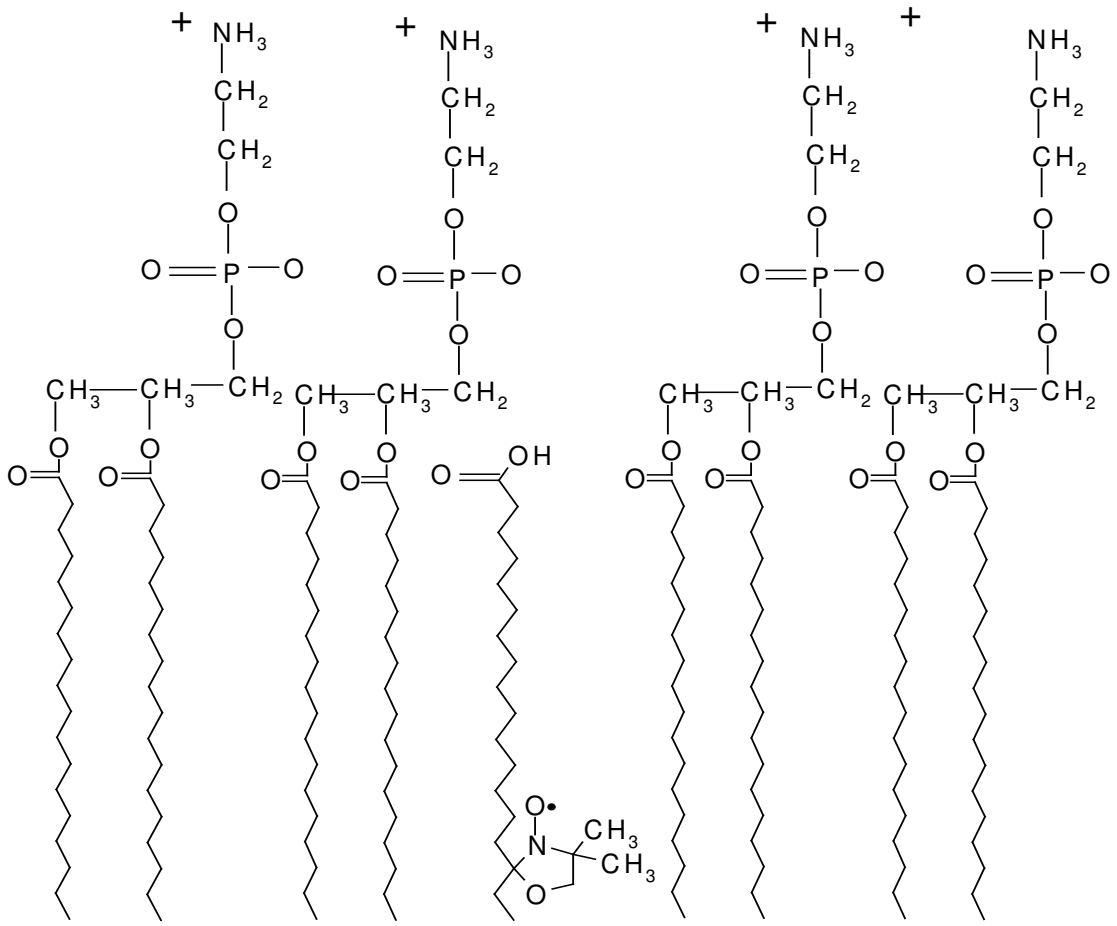

Figure 3.7: A diagram depicting the acyl chain with the nitroxide moiety attached at the 16th carbon. This diagram is a representation of one leaflet of the bilayer. So, this is either the Trans or the Cis side of the membrane.

This lipophilic quencher has its nitroxide moiety located approximately in the middle of the bilayer and so should preferentially quench any labeled residues buried deep in the membrane core (figure 3.7). As can be seen in figure 3.6 and 3.8, all labeled mutants from H95C to F109C are quenched by 5- and 16-doxyl stearic acid.

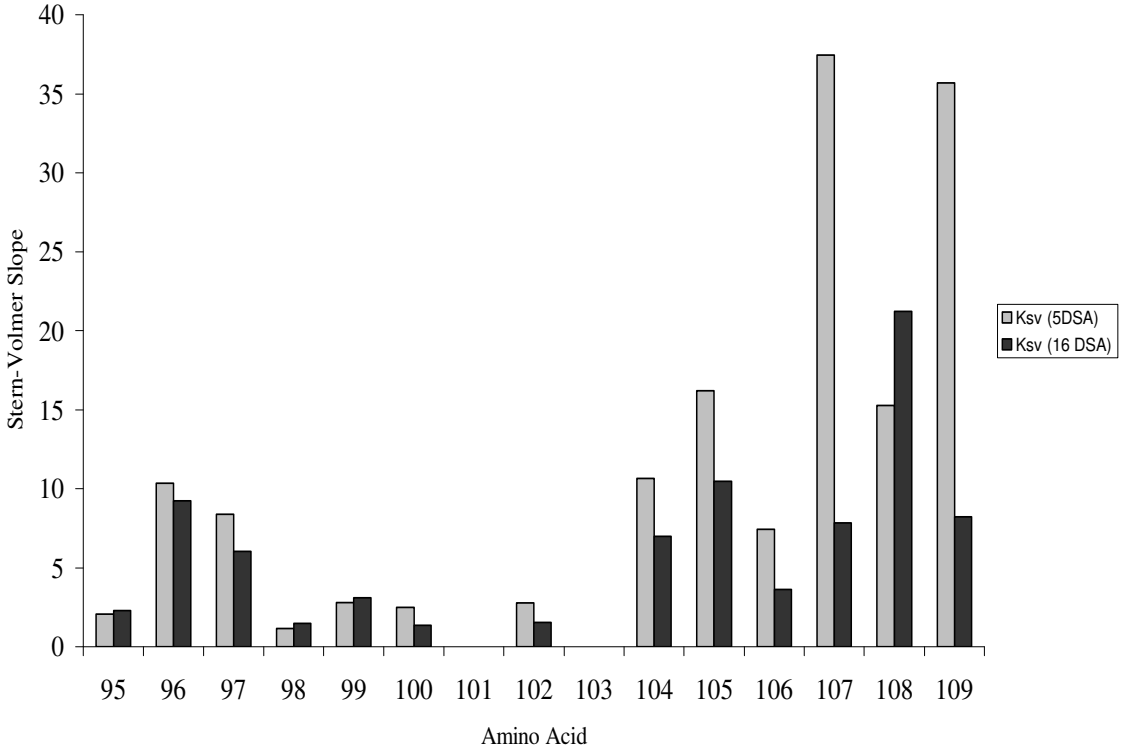

Figure 3.8: Comparison between 5 and 16 Doxyl Stearic Acid quenching of NBD-labeled CAMP factor mutants. Notice the higher degree of quenching with 5 DSA as opposed to 16 DSA.

Interestingly, 16- and 5-doxyl stearic acid quench residues in the 90's similarly compared to residues between N104C and F109C. We also see the alternating pattern within residues N104C to F109C with the 16 doxyl stearic acid quenching, although mutant G108C breaks that pattern. It is quenched more efficiently by 16- than by 5-doxyl stearic acid. Nevertheless, this quenching assay suggests transition of the mutants into the membrane core as these residues get quenched by the membrane-restricted quenchers.

4.0 Discussion

These studies have demonstrated that upon CAMP factor binding and inserting into a membrane, the stretch of amino acids from T90C to K113C arranges into a conformation that inserts into the membrane. More importantly, three different assays confirm that residues from N104C to F109C superficially insert into the membrane with a β-sheet conformation.

Typically, membrane insertion regions of pore-forming toxins are predicted from their monomer structures. This prediction is then confirmed by cysteine scanning mutagenesis. In the present study, however, since the monomeric or oligomeric structure of CAMP factor is not yet known, a hydropathy plot of the protein was constructed - this gave a hydrophobic region that may likely be the membrane insertion region. So, we studied this stretch of amino acids, from T90C to V115C, using cysteine scanning mutagenesis. With several mutants, hemolytic activity was decreased by cysteine mutagenesis or covalent cysteine labeling, but all mutants retained significant activity and were therefore employed in the subsequent fluorescence studies.

Fluorescence intensity measurements of all mutants indicate that they change environment from a solvent exposed to a more hydrophobic one as indicated by their increase in intensity, figure 3.2 A. This transition is also supported by the blue shifts mutants in this study exhibit, figure 3.1 C. After membrane binding, all these mutants show a reduction in wavelengths by about 10 nm. Subsequent quenching with 5- and 16-doxyl stearic acid confirmed that this change in environment is a result of the dye, and thus the residues, moving into the hydrophobic core of the bilayer. While mutants studied by Shanshan Liu also exhibit increased intensity, their shifts were not recorded,

but like mutants in this study, they do contact the membrane as they were quenched by 5- - doxyl stearic acid.

Although all tested mutants were quenched by 5- and 16-doxyl stearic acid, they are quenched more so by 5- than 16-doxyl stearic acid. When one examines figure 3.2 A, it is apparent that residues in the 90's region are quenched to the same extent by 5- and 16- doxyl stearic acid. But from N104C to F109C, 5 doxyl stearic acid is more efficient. This suggests that residues in the 90's insert deeper into the membrane. For the residues to be quenched to the same extent by both quenchers, they would have to insert deep enough to collide with the deeply residing quencher, but shallow enough that they are also within the vicinity of the superficial quencher - perhaps halfway between both quenchers. On the other hand, residues N104C to F109C are closer to the 5- doxyl group and so are quenched less by 16 doxyl stearic acid, implying a superficial residence.

Unlike the other residues, mutant G108C behaves anomalously; in solution, it has a wavelength of about 526 nm. When bound to membrane, it retains this wavelength, suggesting hydrophobic residence before and after membrane binding, yet it exhibits intensity increase after membrane binding. In the intensity difference, 5-doxyl stearic acid and lifetime assays, it is one of the alternating residues, behaving ideally and coherently with the pattern observed. However, it is quenched more strongly by 16-doxyl stearic acid and thus breaks the alternating pattern. More tests would have to be done on this mutant to make conclusions or disprove this anomaly.

Based on results from previously studied membrane damaging cytotoxins, membrane-inserting regions may adopt either α-structure or β-structure. Membrane-interactive amphipathic α-helices and β-strands are characterized by the periodicity of the

interaction of their side chains with the membrane and aqueous environments; approximately every 3.6 residues of an amphipathic α-helix interacts with the membrane (*56*), whereas alternating residues of an amphipathic β-strand interact with the membrane (*49*).

When one examines figure 3.1 C, one notices that residues that form the alternating region, the residues that face the membrane core show about 20 nm blue shifts while those that will face the channel and thus be exposed to water show reductions of about 10 nm. These same residues, those that face the membrane, show the highest change in intensity figure 3.2 A, and highest quenching figure 3.8. To confirm this pattern, we chose to measure the lifetimes (reasons outlined in the results section) of the residues in this region. What we see after the lifetime measurements is the same alternating pattern within residues N104C to F109C. In the work by Shatursky *et al*., (*49*) a similar alternating pattern was observed for a region of the toxin on which work was done. In this work however, while the hydrophobic resides that face the lipid membrane display a very high increase in intensity, the intervening hydrophilic residues show very little or no intensity increase at all. The authors concluded that this alternating pattern reflects a β-sheet conformation, and that the corresponding sequence motif is the means by which this toxin, perfringolysin O, (PFO) penetrates the membrane. Since this same pattern is observed in CAMP factor from residues N104C to F109C, we can also conclude that this region inserts with a β-sheet conformation. However, in CAMP factor, both the hydrophobic and hydrophilic residues in the alternating region all exhibit intensity increase, with the hydrophobic residues having the highest change. Given that the hydrophobic and hydrophilic residues all show some extent of intensity increase and

quenching with both 5- and 16-Doxyl stearic acid, the residence of this region is most likely that shown in figure 4.1

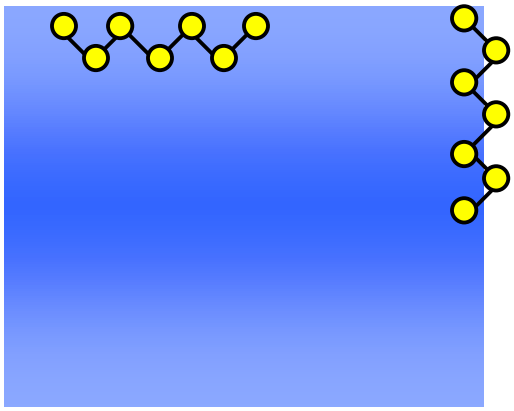

Figure 4.1: Possible membrane interacting pattern of residues N104C to F109C of CAMP factor

where the residues position themselves on the surface of the membrane in a β-sheet structure, thus, all residues having some extent of exposure to both quenchers. The results of this study, together with the foregoing work by Shanshan Liu, represent the first characterization of a membrane-penetrating domain of CAMP factor. The possible role of additional domains in this toxin molecule is currently under investigation.

Appendix A, Spectra of NBD Labeled Mutants T90C to V115C

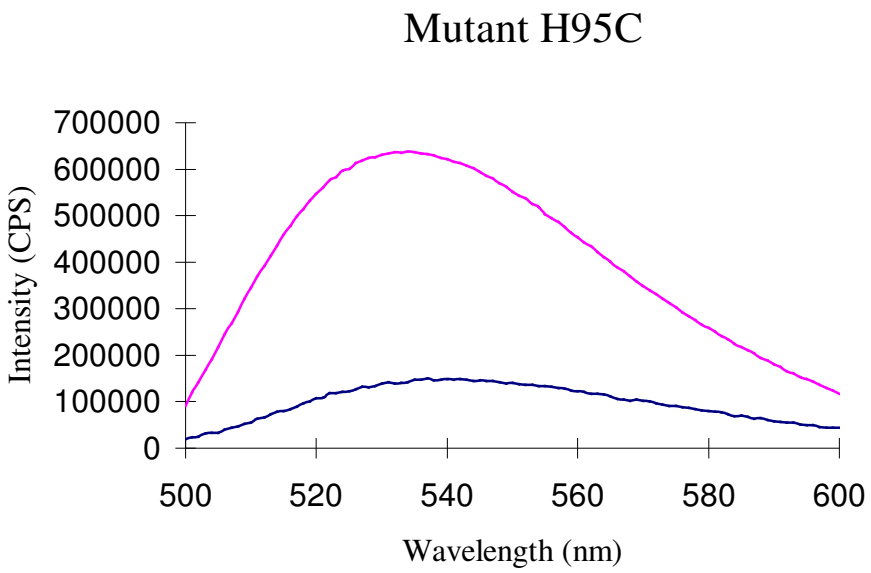

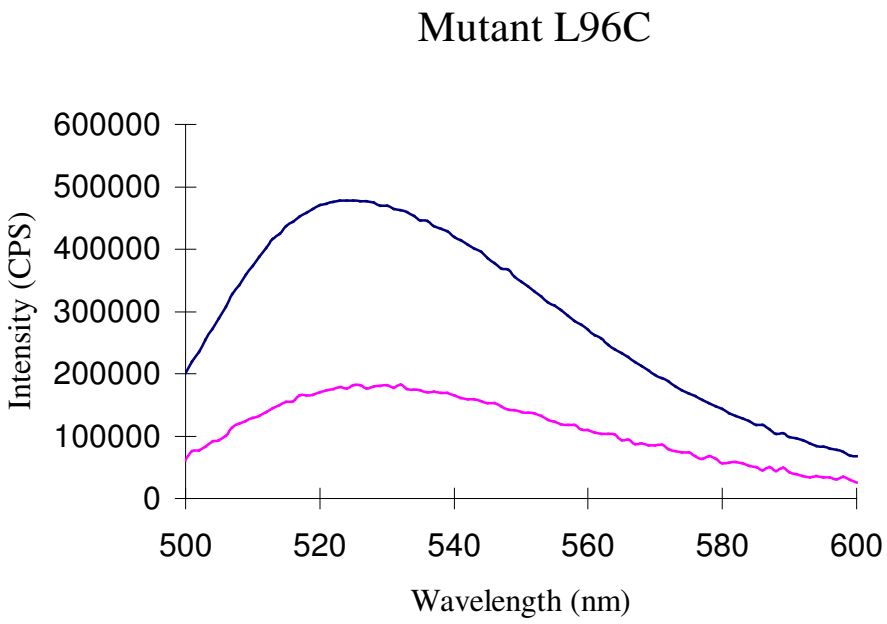

Mutant A97C

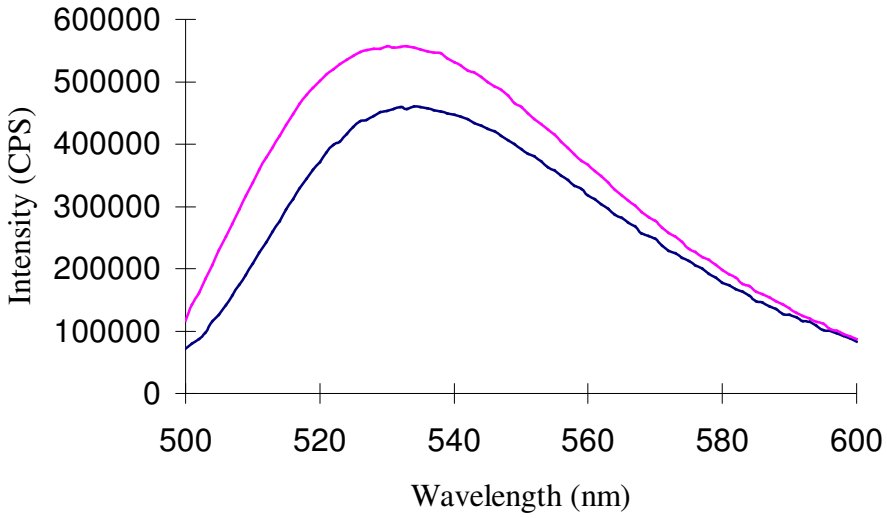

Mutant N98C

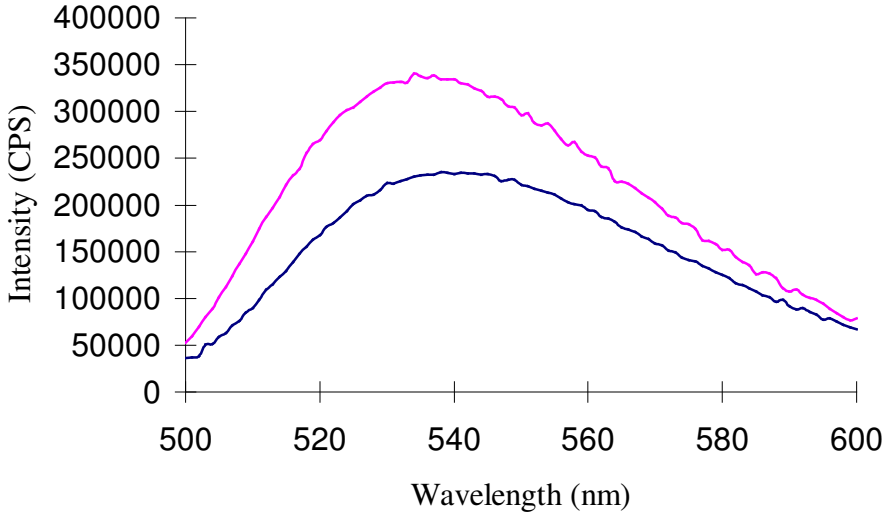

Mutant K99C

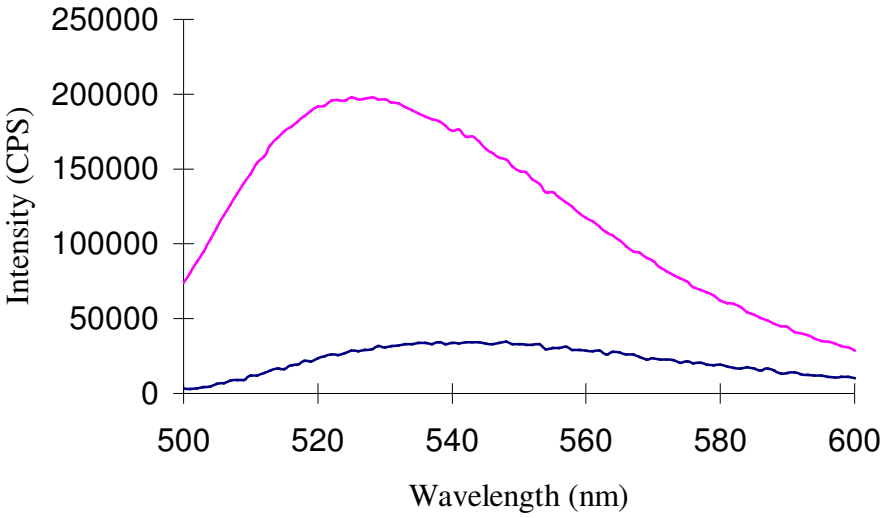

Mutant V100C

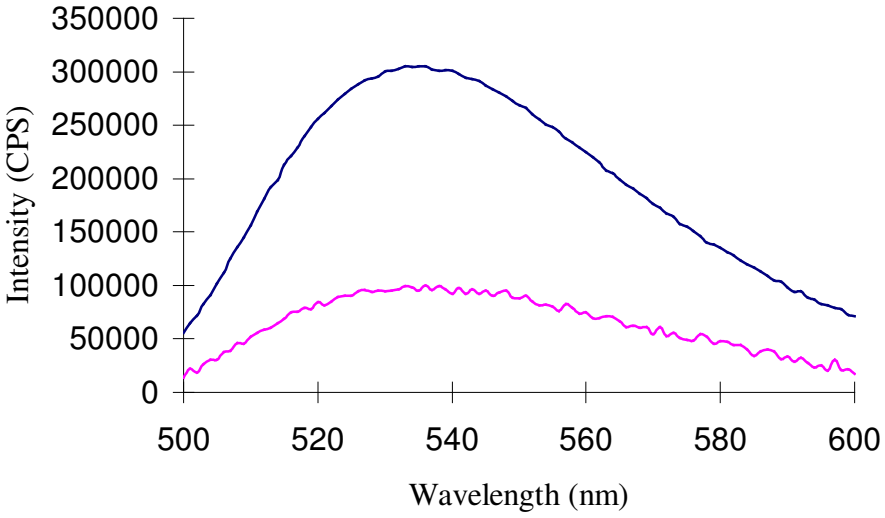

Mutant Q102C

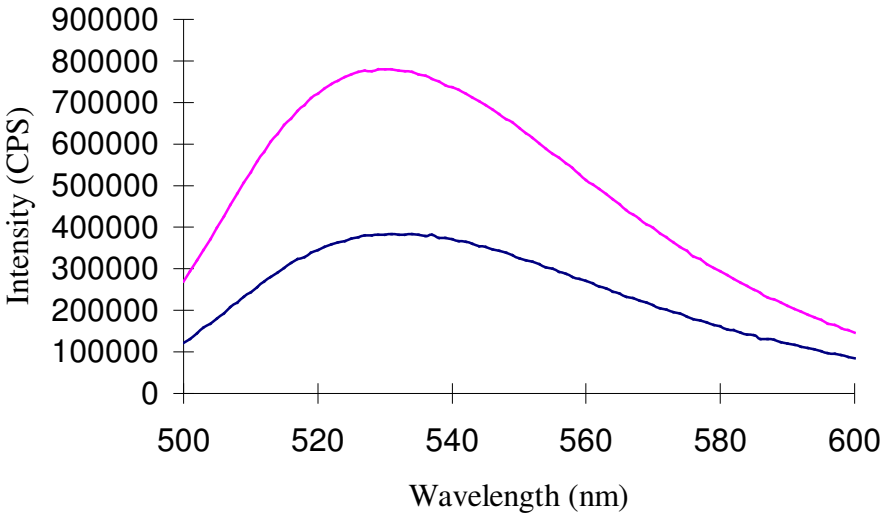

Mutant N104C

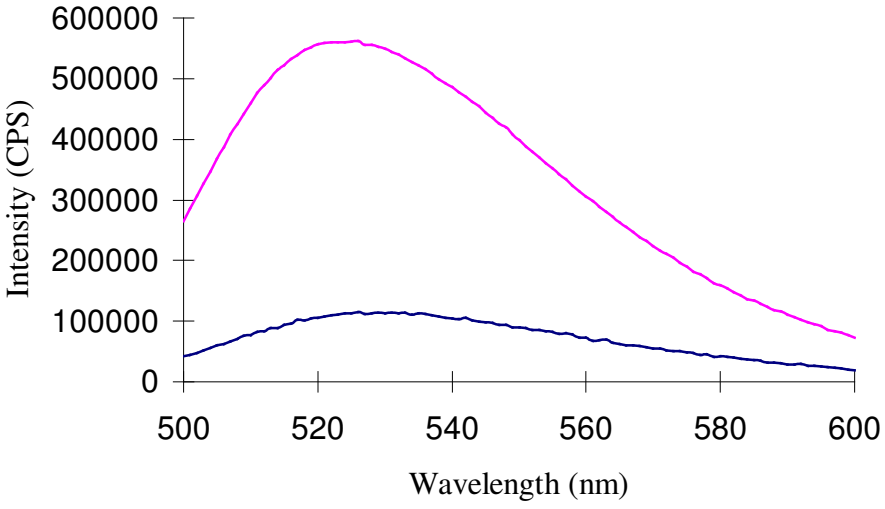

Mutant I105C

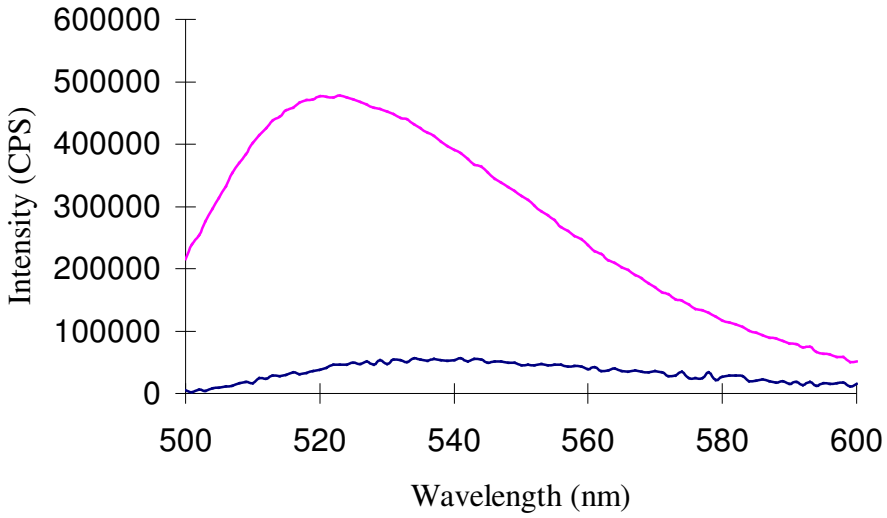

Mutant D106C

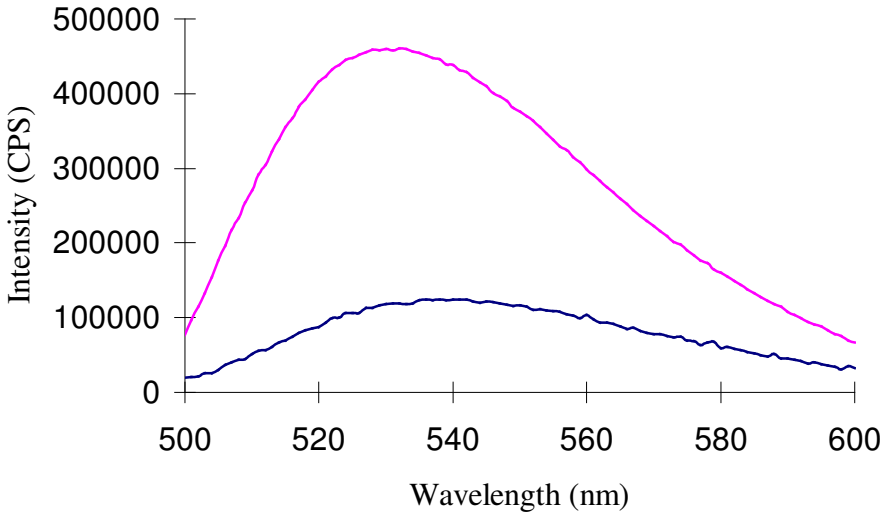

Mutant L107C

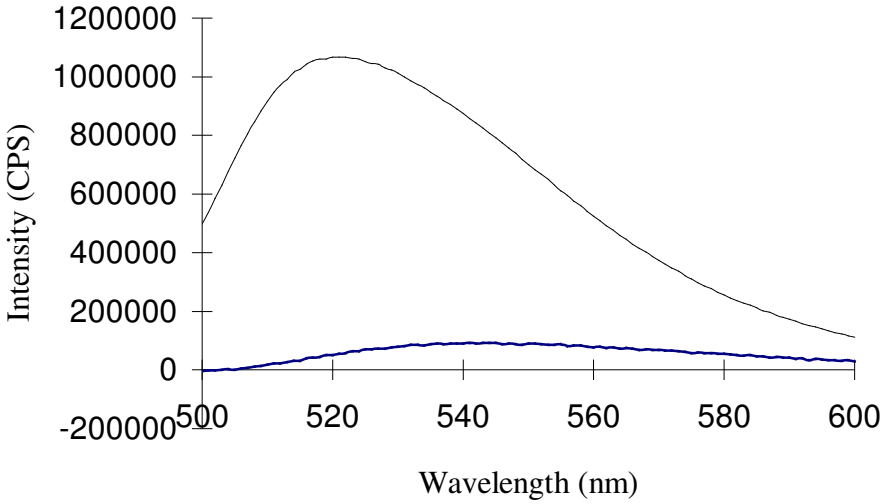

Mutant G108C

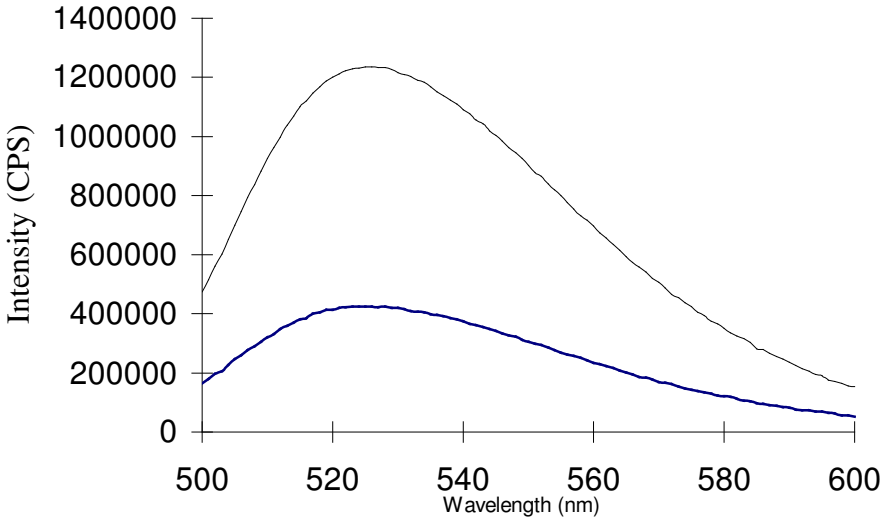

Mutant F109C

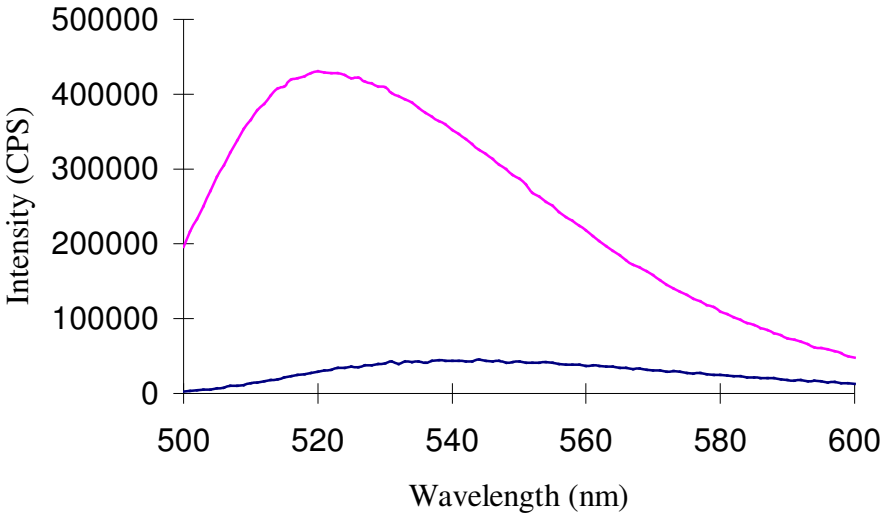

Appendix B, Stern-Volmer plots of 5 and 16 Doxyl Stearic Acid Quenched ^{NBD} labeled Mutants H95C to F109C

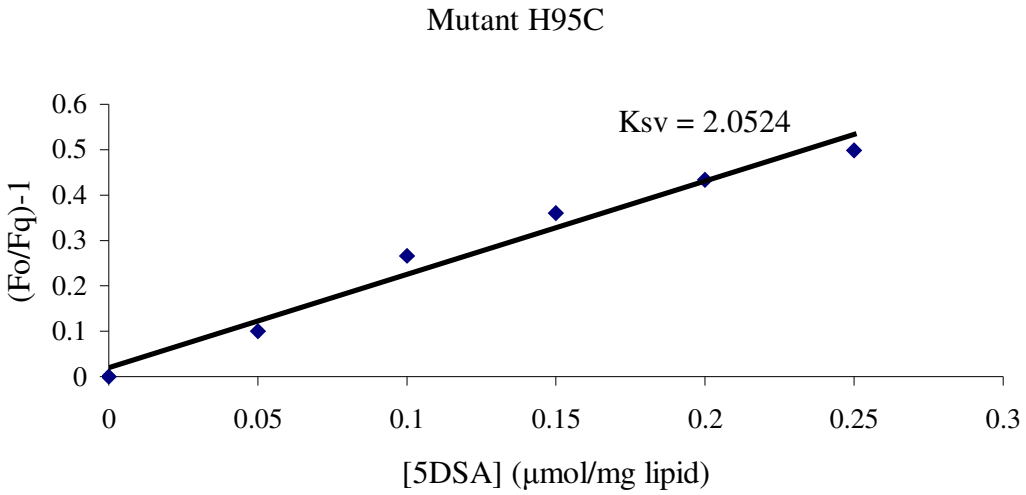

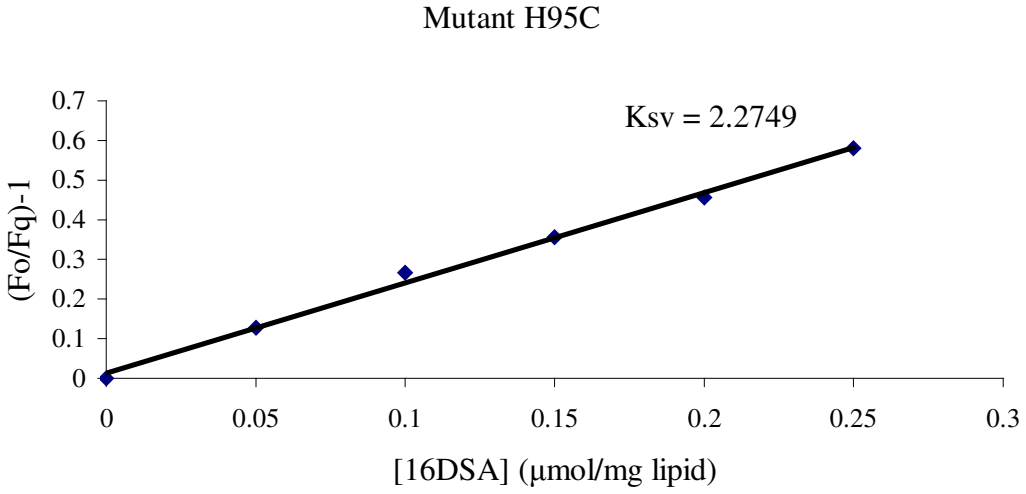

Mutant L96C

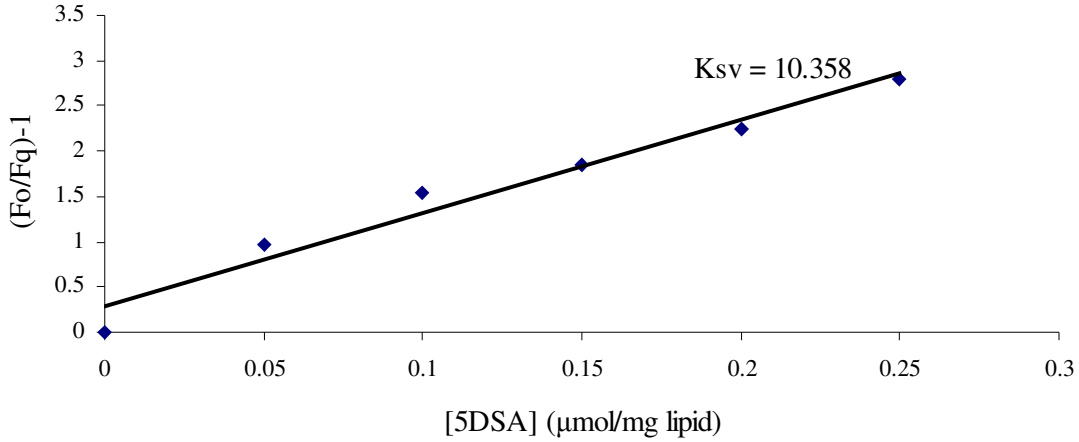

Mutant L96C

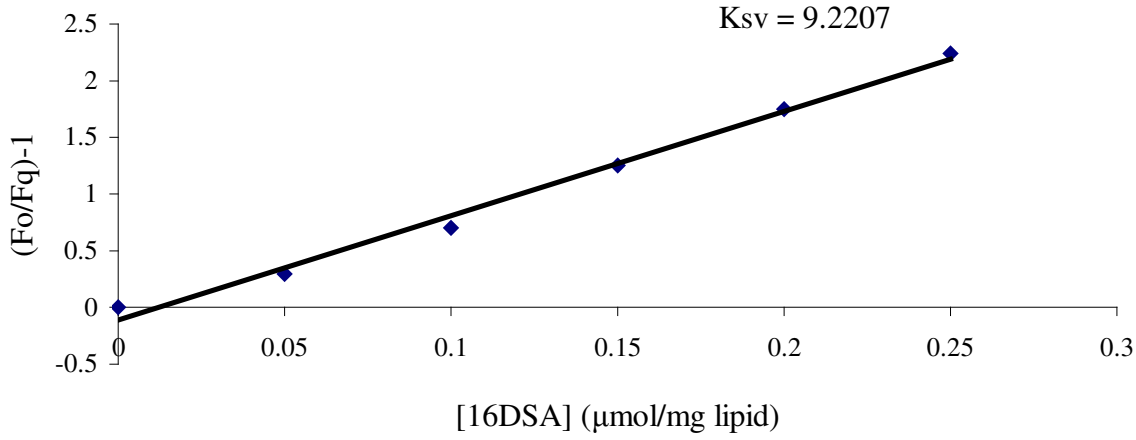

Mutant A97C

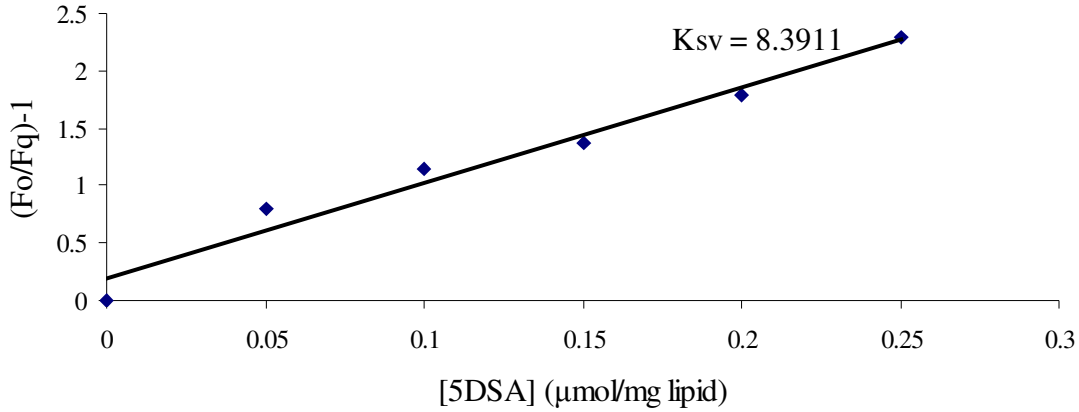

Mutant A97C

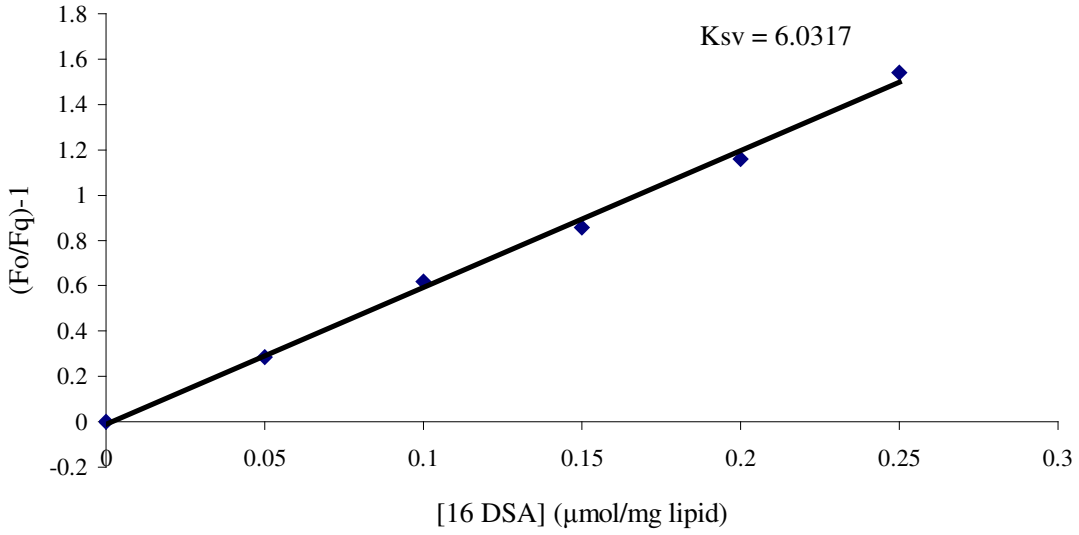

Mutant N98C

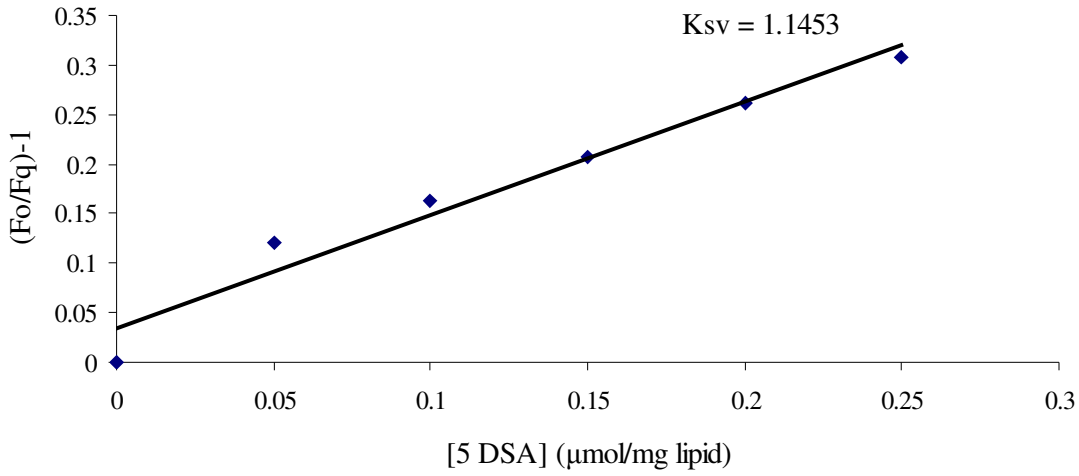

Mutant N98C

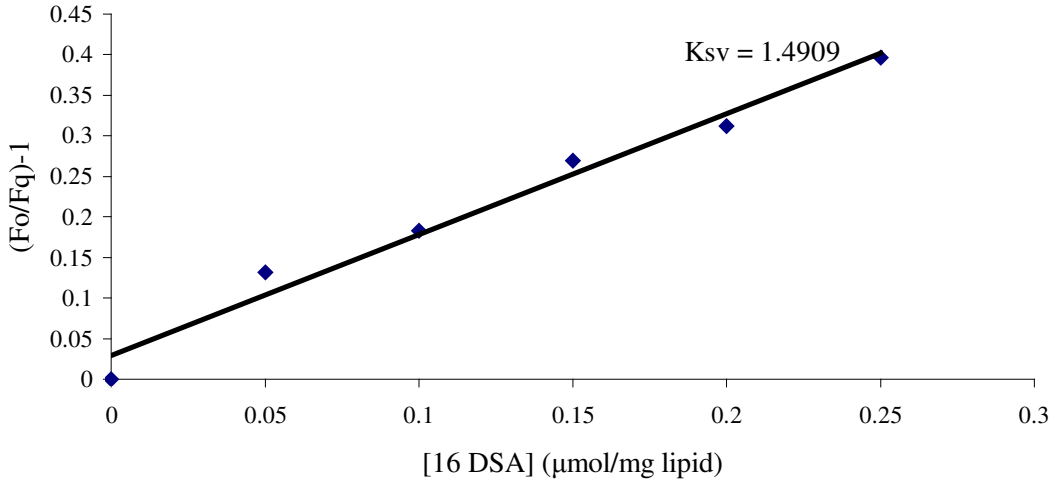

Mutant K99C

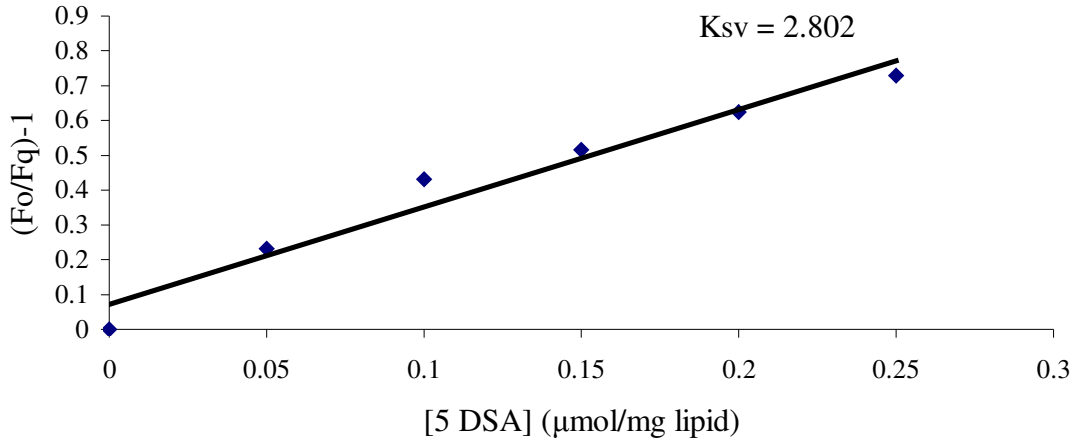

Mutant K99C

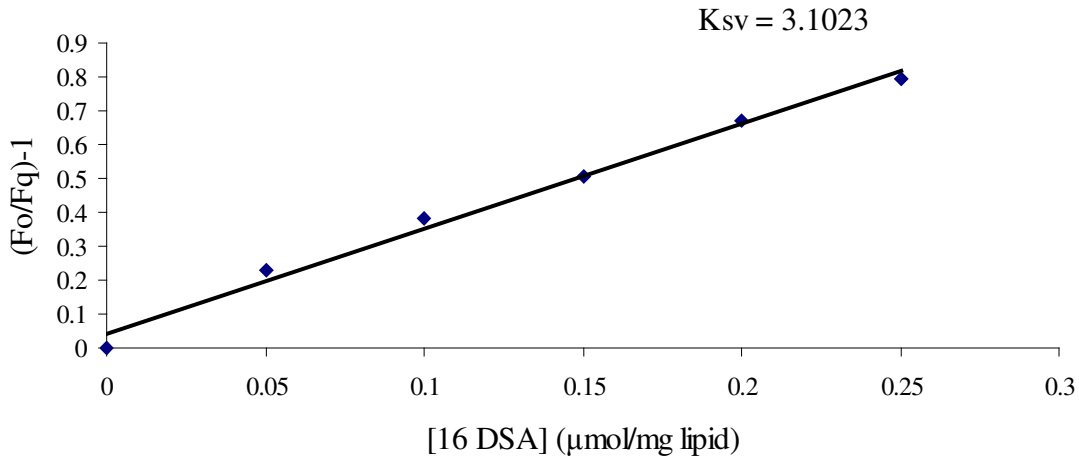

Mutant V100C

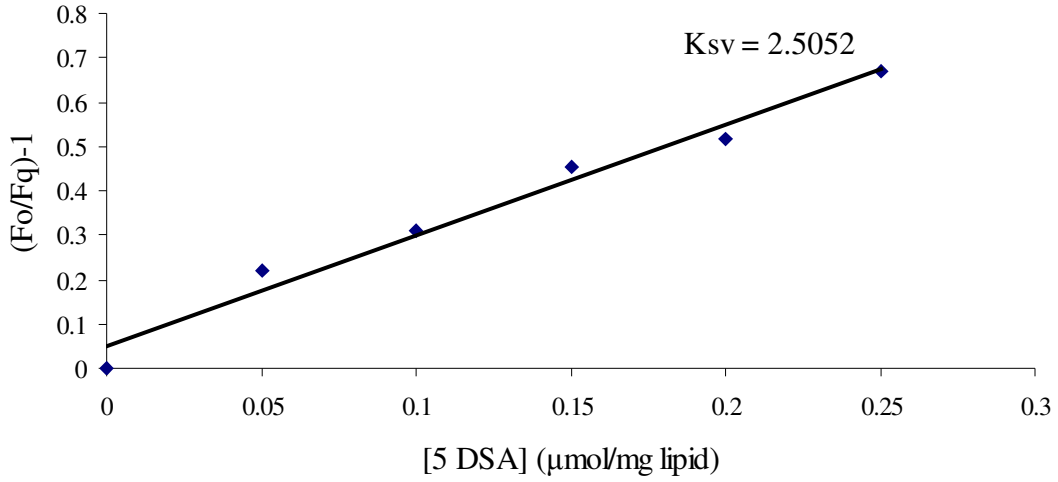

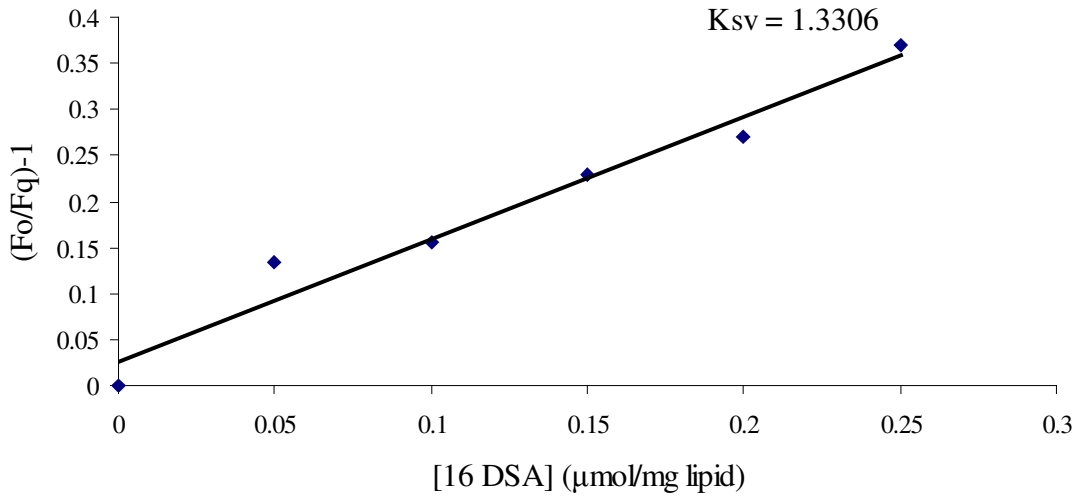

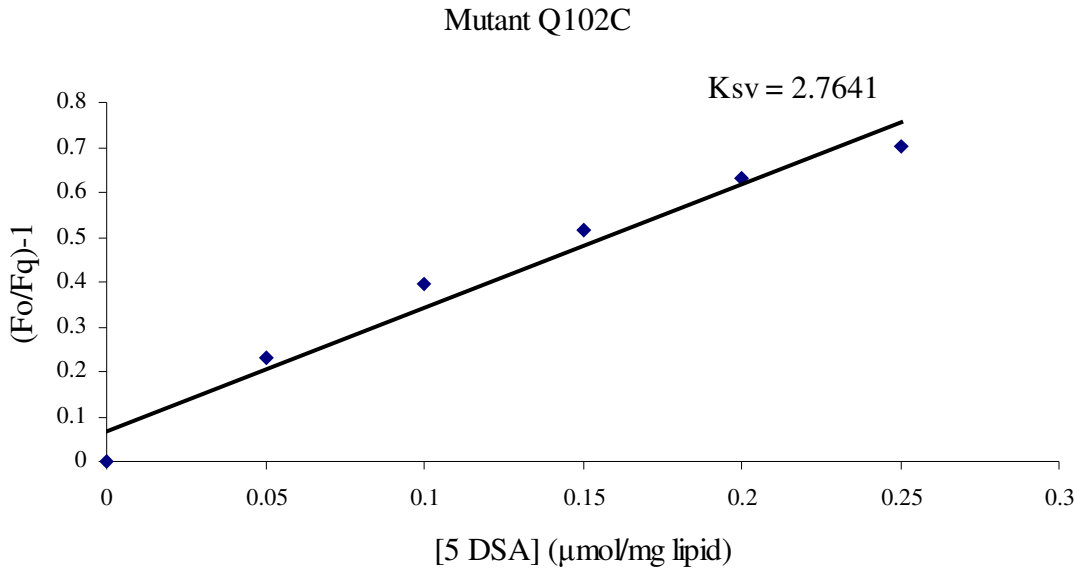
Mutant Q102C
Ksv = 2.7641
(Fo/Fq)-1
0.8
0.7
0.6
0.5
0.4
0.3
0.2
0.1
0
0
0.05
0.1
0.15
0.2
0.25
0.3
[5 DSA] (µmol/mg lipid)

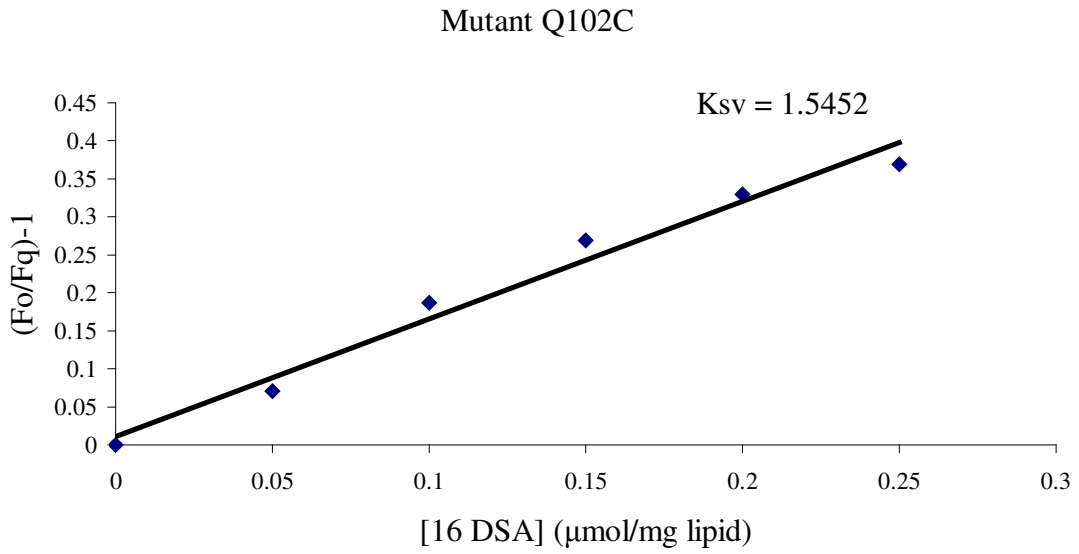
Mutant Q102C
Ksv = 1.5452
(Fo/Fq)-1
0.45
0.4
0.35
0.3
0.25
0.2
0.15
0.1
0.05
0
0
0.05
0.1
0.15
0.2
0.25
0.3
[16 DSA] (µmol/mg lipid)

Mutant N104C

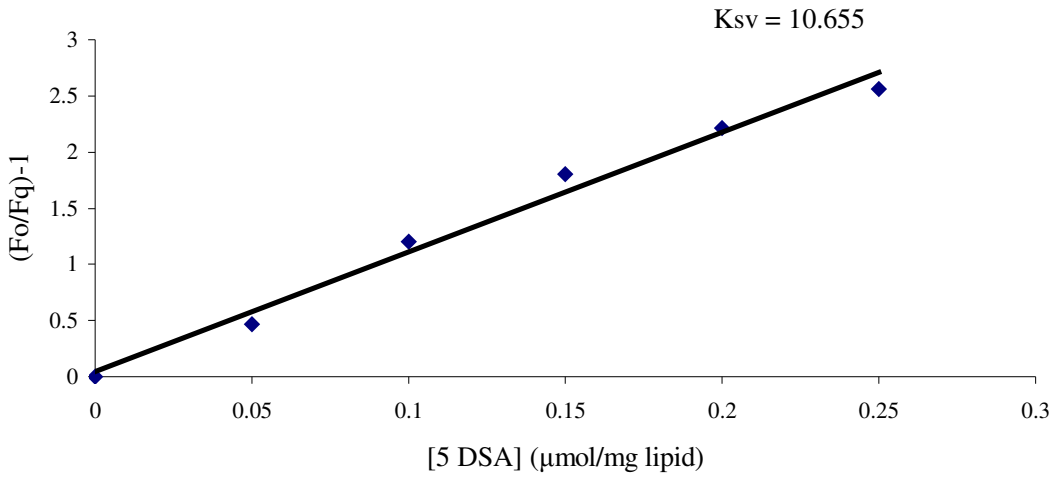

Mutant N104C

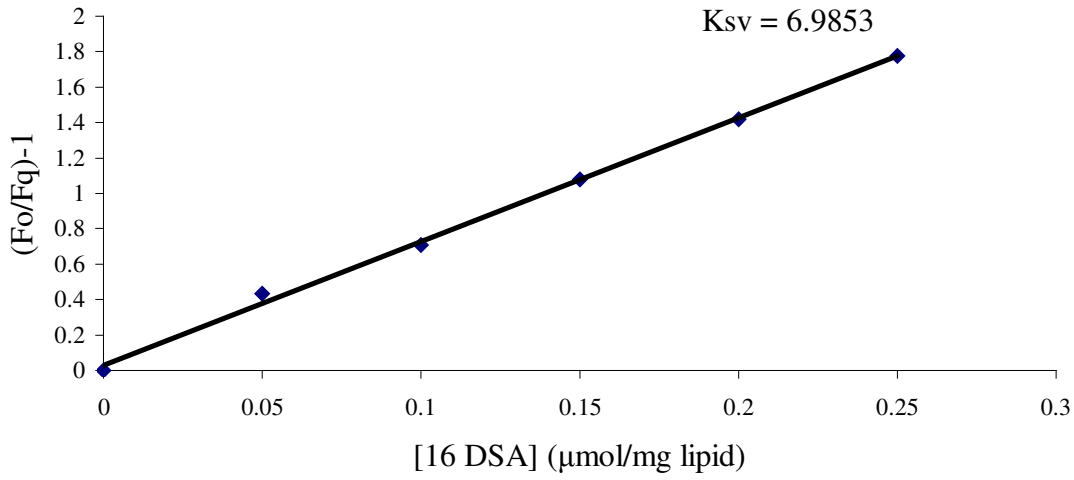

Mutant I105C

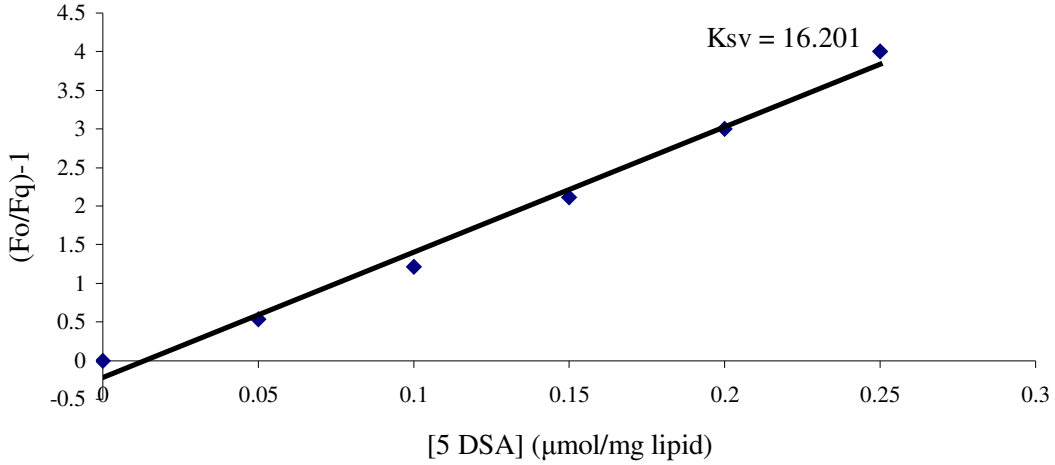

Mutant I105C

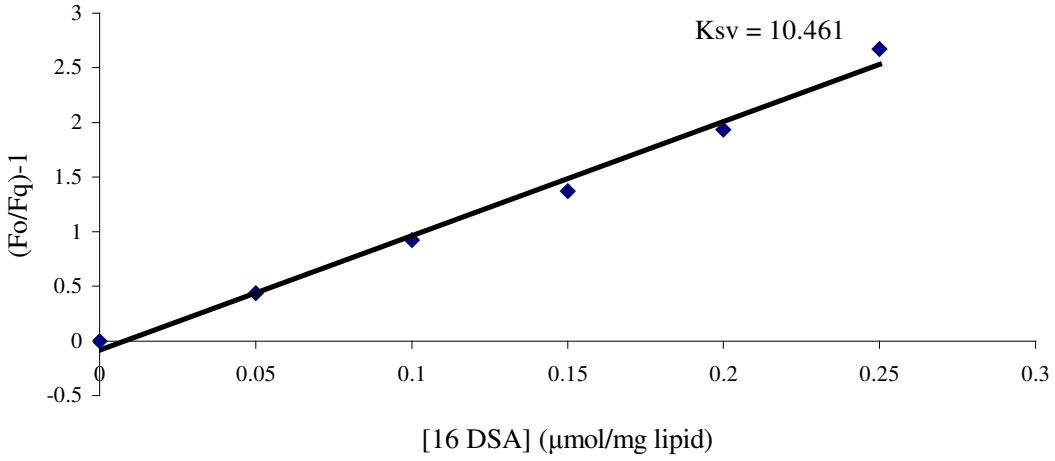

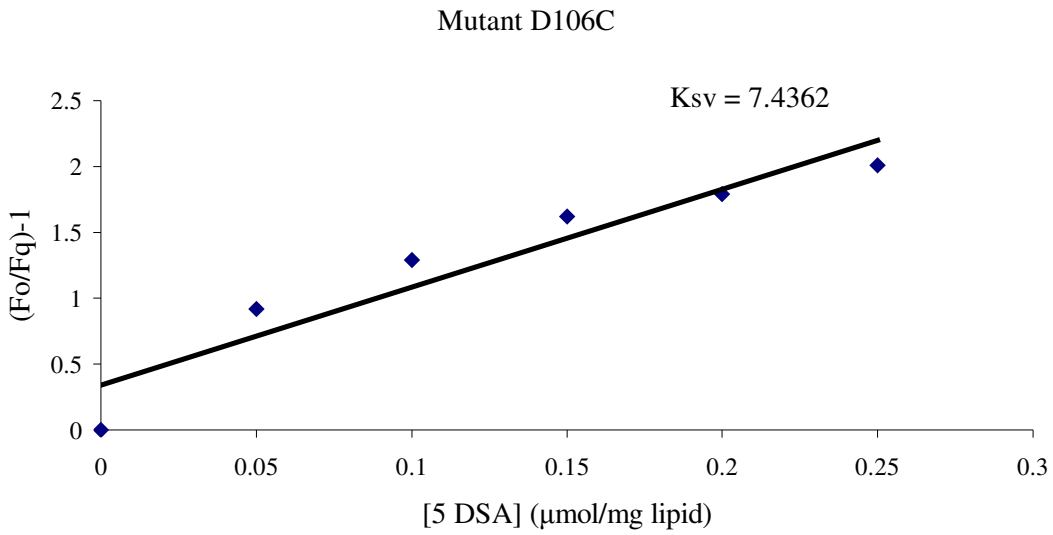
Mutant D106C
Ksv = 7.4362
(Fo/Fq)-1
2.5
2
1.5
1
0.5
0
0
0.05
0.1
0.15
0.2
0.25
0.3
[5 DSA] (µmol/mg lipid)

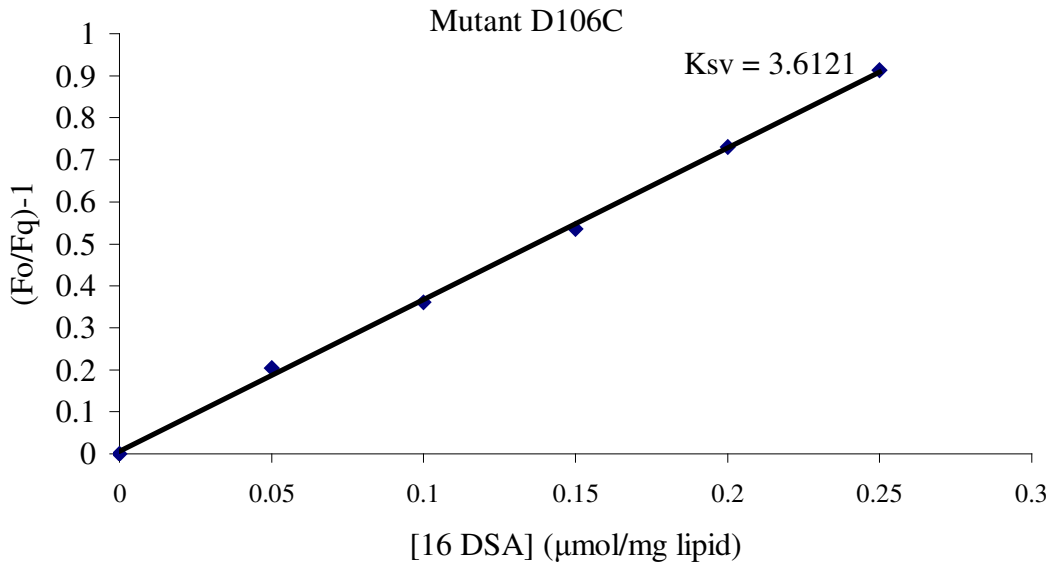
Mutant D106C
Ksv = 3.6121
(Fo/Fq)-1
1
0.9
0.8
0.7
0.6
0.5
0.4
0.3
0.2
0.1
0
0
0.05
0.1
0.15
0.2
0.25
0.3
[16 DSA] (µmol/mg lipid)

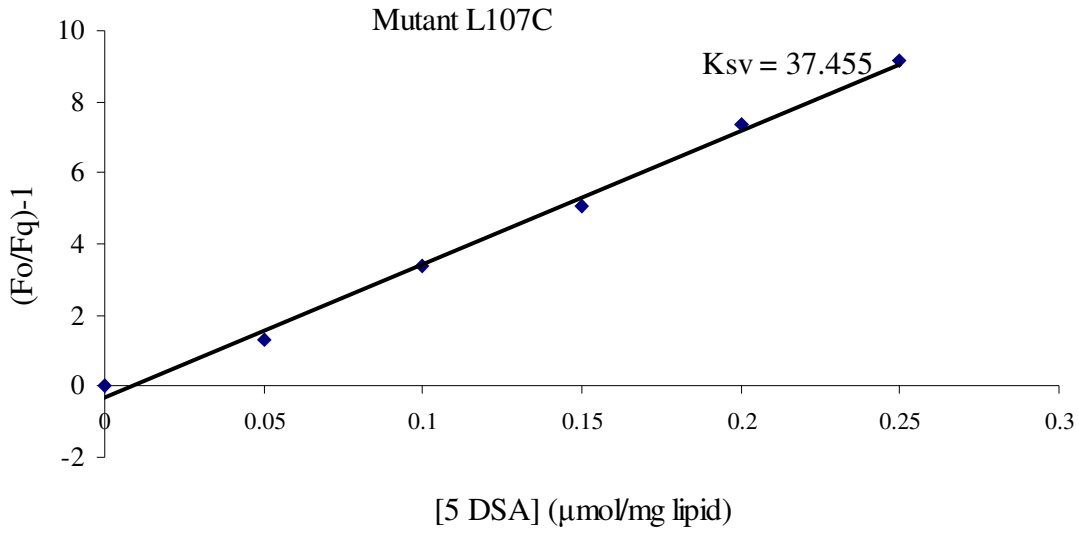
Mutant L107C
Ksv = 37.455
(Fo/Fq)-1
10
8
6
4
2
0
-2
0
0.05
0.1
0.15
0.2
0.25
0.3
[5 DSA] (µmol/mg lipid)

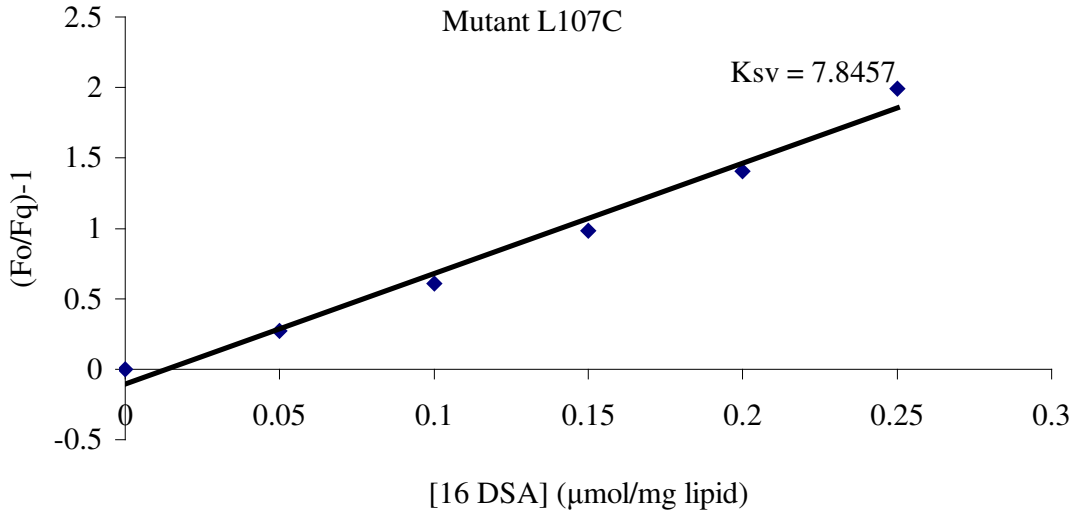
Mutant L107C
Ksv = 7.8457
(Fo/Fq)-1
2.5
2
1.5
1
0.5
0
-0.5
0
0.05
0.1
0.15
0.2
0.25
0.3
[16 DSA] (µmol/mg lipid)

Mutant G108C

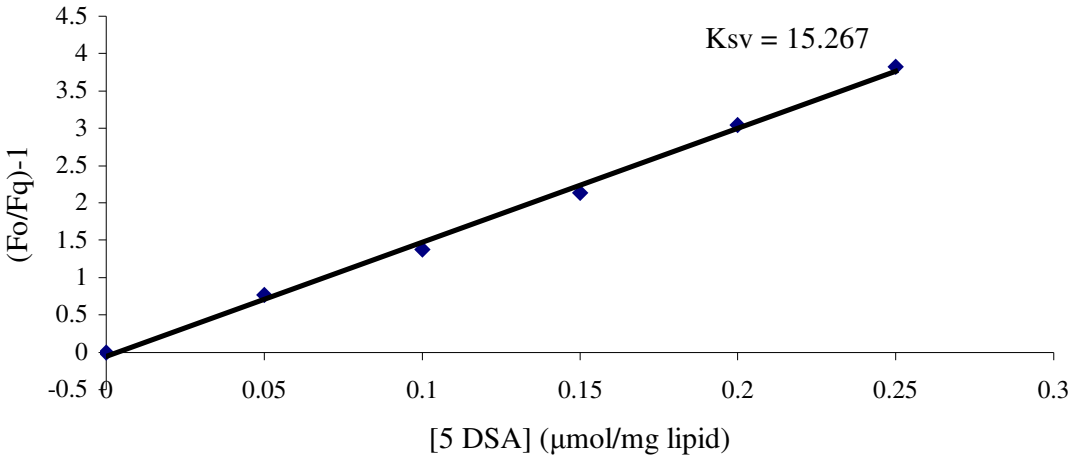

Mutant G108C

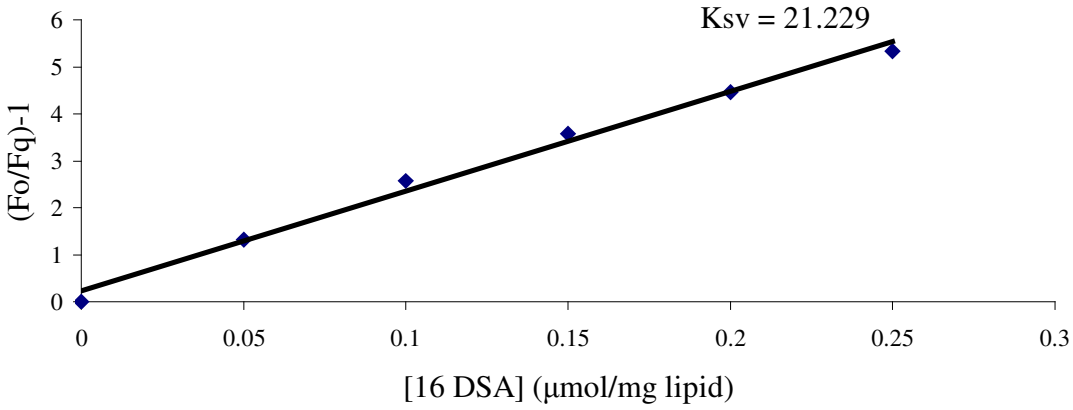

Mutant F109C

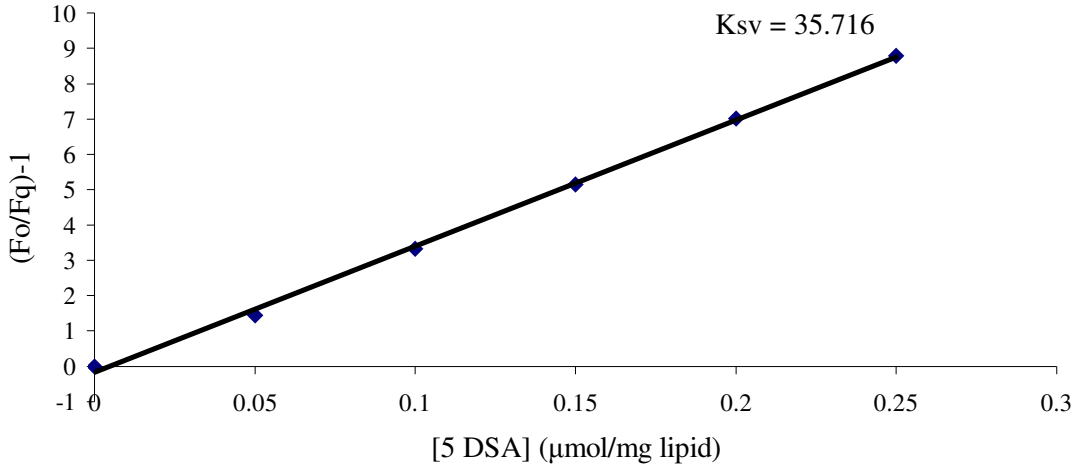

Mutant F109C

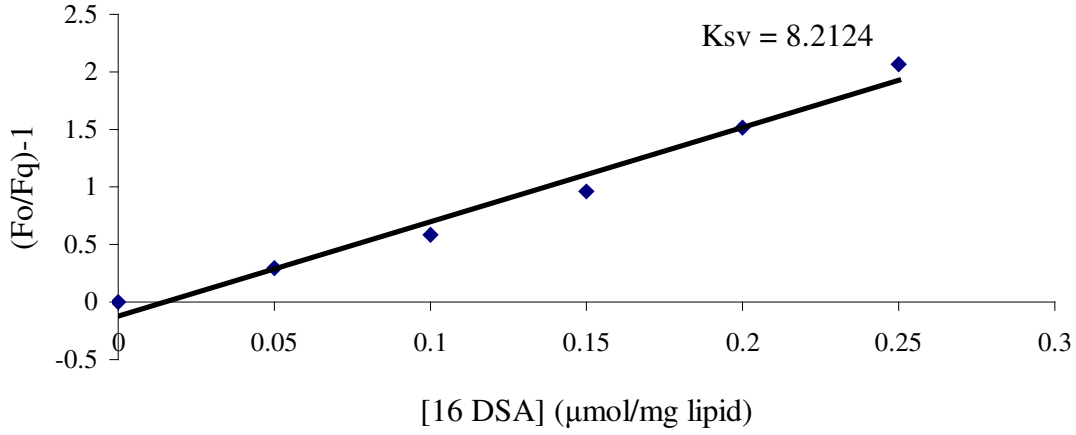

References

(1) Keefe, G. P. (1997) Streptococcus agalactiae mastitis: a review. *The Canadian veterinary journal. La revue veterinaire canadienne 38*, 429-37.

(2) Christie, R., Atkins , N., and Munch-Peterson, E. (1944) A note on a lytic phenomenon shown by group B streptococci. *Aust J Exp Biol 22*, 197-200.

(3) Darling, C. L. (1975) Standardization and evaluation of the CAMP reaction for the prompt, presumptive identification of Streptococcus agalactiae (Lancefield group B) in clinical material. *Journal of clinical microbiology 1*, 171-4.

(4) Phillips, E. A., Tapsall, J. W., and Smith, D. D. (1980) Rapid tube CAMP test for identification of Streptococcus agalactiae (Lancefield group B). *J Clin Microbiol 12*, 135-7.

(5) Barton, L. L., Feigin, R. D., and Lins, R. (1973) Group B beta hemolytic streptococcal meningitis in infants. *The Journal of pediatrics 82*, 719-23.

(6) Bernheimer, A. W., Linder, R., and Avigad, L. S. (1979) Nature and mechanism of action of the cAMP protein of group B streptococci. *Infection and Immunity 23*, 838-44.

(7) Jurgens, D., Shalaby, F. Y., and Fehrenbach, F. J. (1985) Purification and characterization of cAMP-factor from Streptococcus agalactiae by hydrophobic interaction chromatography and chromatofocusing. *J Chromatogr FIELD Full Journal Title:Journal of chromatography 348*, 363-70.

(8) Sterzik, B., and Fehrenbach, F. J. (1985) Reaction components influencing CAMP factor-induced lysis. *Journal of General Microbiology 131*, 817-20.

(9) Lang, S., and Palmer, M. (2003) Characterization of Streptococcus agalactiae CAMP Factor as a Pore-forming Toxin. *Journal of Biological Chemistry 278*, 38167-38173.

(10) Goot, F. (2001) Pore-Forming toxins. *New York, NY: Sringer* 165-200

(11) Gilbert, R. J. C. (2002) Pore-forming toxins. *Cellular and Molecular Life Sciences 59*, 832-844.

(12) Arbuthnott, J. (1982) Bacterial cytolysins (membrane damagiing toxins). *Elsevier*.

(13) Alouf, J., and Freer , J. (1999) The comprehensive sourcebook of bacterial protein toxins. *San Diego: Academic Press Second Edition*.

(14) Bhakdi, S., Weller, U., Walev, I., Martin, E., Jonas, D., and Palmer, M. (1993) A guide to the use of pore-forming toxins for controlled permeabilization of cell membranes. *Medical Microbiology and Immunology 182*, 167-75.

(15) Dunn, L. A., and Holz, R. W. (1983) Catecholamine secretion from digitonin-treated adrenal medullary chromaffin cells. *J Biol Chem 258*, 4989-93.

(16) Ahnert-Hilger, G., Bhakdi, S., and Gratzl, M. (1985) Minimal requirements for exocytosis. A study using PC 12 cells permeabilized with staphylococcal alpha-toxin. *The Journal of biological chemistry 260*, 12730-4.

(17) Yang, W. S., Park, S. O., Yoon, A. R., Yoo, J. Y., Kim, M. K., Yun, C. O., and Kim, C. W. (2006) Suicide cancer gene therapy using pore-forming toxin, streptolysin O. *Mol Cancer Ther 5*, 1610-9.

(18) Gazit, E., La Rocca, P., Sansom, M. S., and Shai, Y. (1998) The structure and organization within the membrane of the helices composing the pore-forming domain of Bacillus thuringiensis delta-endotoxin are consistent with an "umbrella-like" structure of the pore. *Proc Natl Acad Sci U S A 95*, 12289-94.
(19) Bravo, A., Gill, S. S., and Soberon, M. (2007) Mode of action of Bacillus thuringiensis Cry and Cyt toxins and their potential for insect control. *Toxicon 49*, 423-35.
(20) Hughson, F. M. (1997) Penetrating insights into pore formation. *Nature structural biology 4*, 89-92.
(21) Gouaux, E. (1997) Channel-forming toxins: tales of transformation. *Current Opinion in Structural Biology 7*, 566-573.
(22) Alouf, J., and Popoff, M. (2006) The Comprehensive Sourcebook of Bacterial Protein Toxins.
(23) Song, L., Hobaugh, M. R., Shustak, C., Cheley, S., Bayley, H., and Gouaux, J. E. (1996) Structure of staphylococcal alpha-hemolysin, a heptameric transmembrane pore. *Science 274*, 1859-66.
(24) Li, J., Koni, P. A., and Ellar, D. J. (1996) Structure of the mosquitocidal delta-endotoxin CytB from Bacillus thuringiensis sp. kyushuensis and implications for membrane pore formation. *J Mol Biol 257*, 129-52.
(25) Hofte, H., and Whiteley, H. R. (1989) Insecticidal crystal proteins of Bacillus thuringiensis. *Microbiol Rev 53*, 242-55.
(26) Hofmann, C., Vanderbruggen, H., Hofte, H., Van Rie, J., Jansens, S., and Van Mellaert, H. (1988) Specificity of Bacillus thuringiensis delta-endotoxins is correlated with the presence of high-affinity binding sites in the brush border membrane of target insect midguts. *Proc Natl Acad Sci U S A 85*, 7844-8.
(27) Armstrong, J. L., Rohrmann, G. F., and Beaudreau, G. S. (1985) Delta endotoxin of Bacillus thuringiensis subsp. israelensis. *J Bacteriol 161*, 39-46.
(28) Promdonkoy, B., and Ellar, D. J. (2003) Investigation of the pore-forming mechanism of a cytolytic delta-endotoxin from Bacillus thuringiensis. *Biochem J 374*, 255-9.
(29) Promdonkoy, B., and Ellar, D. J. (2000) Membrane pore architecture of a cytolytic toxin from Bacillus thuringiensis. *Biochem J 350 Pt 1*, 275-82.
(30) Li, J., Derbyshire, D. J., Promdonkoy, B., and Ellar, D. J. (2001) Structural implications for the transformation of the Bacillus thuringiensis delta-endotoxins from water-soluble to membrane-inserted forms. *Biochem Soc Trans 29*, 571-7.
(31) Tilley, S. J., and Saibil, H. R. (2006) The mechanism of pore formation by bacterial toxins. *Current Opinion in Structural Biology 16*, 230-236.
(32) Kawate, T., and Gouaux, E. (2003) Arresting and releasing Staphylococcal alpha-hemolysin at intermediate stages of pore formation by engineered disulfide bonds. *Protein Sci 12*, 997-1006.
(33) Menestrina, G., Dalla Serra, M., Comai, M., Coraiola, M., Viero, G., Werner, S., Colin, D. A., Monteil, H., and Prevost, G. (2003) Ion channels and bacterial infection: the case of beta-barrel pore-forming protein toxins of Staphylococcus aureus. *FEBS Lett 552*, 54-60.
(34) Guillet, V., Roblin, P., Werner, S., Coraiola, M., Menestrina, G., Monteil, H., Prevost, G., and Mourey, L. (2004) Crystal structure of leucotoxin S component:

new insight into the Staphylococcal beta-barrel pore-forming toxins. *J Biol Chem 279*, 41028-37.
(35) Tweten, R. K. (2005) Cholesterol-dependent cytolysins, a family of versatile pore-forming toxins. *Infect Immun 73*, 6199-209.
(36) Weis, S., and Palmer, M. (2001) Streptolysin O: the C-terminal, tryptophan-rich domain carries functional sites for both membrane binding and self-interaction but not for stable oligomerization. *Biochim Biophys Acta 1510*, 292-9.
(37) Wu, Z., Jakes, K. S., Samelson-Jones, B. S., Lai, B., Zhao, G., London, E., and Finkelstein, A. (2006) Protein translocation by bacterial toxin channels: a comparison of diphtheria toxin and colicin Ia. *Biophys J 91*, 3249-56.
(38) Gill, D. M. (1978) Seven toxic peptides that cross cell membranes., 291-322.
(39) Hoch, D. H., Romero-Mira, M., Ehrlich, B. E., Finkelstein, A., DasGupta, B. R., and Simpson, L. L. (1985) Channels formed by botulinum, tetanus, and diphtheria toxins in planar lipid bilayers: relevance to translocation of proteins across membranes. *Proc Natl Acad Sci U S A 82*, 1692-6.
(40) Silverman, J. A., Mindell, J. A., Finkelstein, A., Shen, W. H., and Collier, R. J. (1994) Mutational analysis of the helical hairpin region of diphtheria toxin transmembrane domain. *J Biol Chem 269*, 22524-32.
(41) Hayashibara, M., and London, E. (2005) Topography of diphtheria toxin A chain inserted into lipid vesicles. *Biochemistry 44*, 2183-96.
(42) Tortorella, D., Sesardic, D., Dawes, C. S., and London, E. (1995) Immunochemical analysis shows all three domains of diphtheria toxin penetrate across model membranes. *J Biol Chem 270*, 27446-52.
(43) Kachel, K., Ren, J., Collier, R. J., and London, E. (1998) Identifying transmembrane states and defining the membrane insertion boundaries of hydrophobic helices in membrane-inserted diphtheria toxin T domain. *J Biol Chem 273*, 22950-6.
(44) de Maagd, R. A., Bravo, A., Berry, C., Crickmore, N., and Schnepf, H. E. (2003) Structure, diversity, and evolution of protein toxins from spore-forming entomopathogenic bacteria. *Annu Rev Genet 37*, 409-33.
(45) Griffitts, J. S., Haslam, S. M., Yang, T., Garczynski, S. F., Mulloy, B., Morris, H., Cremer, P. S., Dell, A., Adang, M. J., and Aroian, R. V. (2005) Glycolipids as receptors for Bacillus thuringiensis crystal toxin. *Science 307*, 922-5.
(46) Malovrh, P., Viero, G., Serra, M. D., Podlesek, Z., Lakey, J. H., Macek, P., Menestrina, G., and Anderluh, G. (2003) A novel mechanism of pore formation: membrane penetration by the N-terminal amphipathic region of equinatoxin. *J Biol Chem 278*, 22678-85.
(47) Rosconi, M. P., Zhao, G., and London, E. (2004) Analyzing topography of membrane-inserted diphtheria toxin T domain using BODIPY-streptavidin: at low pH, helices 8 and 9 form a transmembrane hairpin but helices 5-7 form stable nonclassical inserted segments on the cis side of the bilayer. *Biochemistry 43*, 9127-39.
(48) Rosconi, M. P., and London, E. (2002) Topography of helices 5-7 in membrane-inserted diphtheria toxin T domain: identification and insertion boundaries of two hydrophobic sequences that do not form a stable transmembrane hairpin. *J Biol Chem 277*, 16517-27.

(49) Shatursky, O., Heuck, A. P., Shepard, L. A., Rossjohn, J., Parker, M. W., Johnson, A. E., and Tweten, R. K. (1999) The mechanism of membrane insertion for a cholesterol-dependent cytolysin: a novel paradigm for pore-forming toxins. *Cell 99*, 293-9.
(50) Shepard, L. A., Heuck, A. P., Hamman, B. D., Rossjohn, J., Parker, M. W., Ryan, K. R., Johnson, A. E., and Tweten, R. K. (1998) Identification of a membrane-spanning domain of the thiol-activated pore-forming toxin Clostridium perfringens perfringolysin O: an alpha-helical to beta-sheet transition identified by fluorescence spectroscopy. *Biochemistry 37*, 14563-74.
(51) Lundblad, R. (1994) Techniques in protein modification. *Boca Raton: CRC Press*, 194-233.
(52) Smith, D. J., Maggio, E. T., and Kenyon, G. L. (1975) Simple alkanethiol groups for temporary blocking of sulfhydryl groups of enzymes. *Biochemistry 14*, 766-71.
(53) Ruhlmann, J., Wittmann-Liebold, B., Jurgens, D., and Fehrenbach, F. J. (1988) Complete amino acid sequence of protein B. *FEBS Lett 235*, 262-6.
(54) Howorka, S., and Bayley, H. (1998) Improved protocol for high-throughput cysteine scanning mutagenesis. *Biotechniques 25*, 764-6, 768, 770 passim.
(55) Palmer, M. (2001) The family of thiol-activated, cholesterol-binding cytolysins. *Toxicon 39*, 1681-9.
(56) Melton, J. A., Parker, M. W., Rossjohn, J., Buckley, J. T., and Tweten, R. K. (2004) The identification and structure of the membrane-spanning domain of the Clostridium septicum alpha toxin. *J Biol Chem 279*, 14315-22.
(57) Fivaz, M., Abrami, L., Tsitrin, Y., and van der Goot, F. G. (2001) Not as simple as just punching a hole. *Toxicon 39*, 1637-45.
(58) Abdel Ghani, E. M., Weis, S., Walev, I., Kehoe, M., Bhakdi, S., and Palmer, M. (1999) Streptolysin O: inhibition of the conformational change during membrane binding of the monomer prevents oligomerization and pore formation. *Biochemistry 38*, 15204-11.
(59) Lakowicz, R. J. (1999) Principles of Fluorescence Spectroscopy. *New York: Kluwer Academic/Plenum Publishers Second Edition*.
(60) Chattopadhyay, A., and London, E. (1987) Parallax method for direct measurement of membrane penetration depth utilizing fluorescence quenching by spin-labeled phospholipids. *Biochemistry 26*, 39-45.
(61) Koriazova, L. K., and Montal, M. (2003) Translocation of botulinum neurotoxin light chain protease through the heavy chain channel. *Nat Struct Biol 10*, 13-8.